UNIVERSITY OF
BIRMINGHAM

BLENDS OF CYCLIC POLY (BUTYLENE TEREPHTHALATE)/ MULTIWALLED CARBON NANOTUBE NANOCOMPOSITES PREPARED BY *IN SITU* POLYMERIZATION

By

YAN ZHANG

A thesis submitted to the University of Birmingham

for the degree of

Master of Research (MRes)

School of Metallurgy and Materials

College of Engineering and Physical Science

University of Birmingham

November 2014

SYNOPSIS

Most polymer materials used currently in industry have high viscosity, so it is difficult to make a composite. But unlike other common polymers, the viscosity of cyclic poly (butylene terephthalate) oligomers (CBT) is like water. This interesting performance gives CBT a promising future in polymer composite production.

It is believed that carbon nanotubes promote high stiffness and strength in materials as they act as a reinforcing filler in nanocomposites.

In this work, multiwalled carbon nanotubes (MWNTs) were blended with cyclic poly (butylene terephthalate) by a new method. The materials were mixed in solid dispersion and prepared by simultaneous in situ polymerisation.

This thesis involves two parts. One part is the thermal behaviour of neat cyclic poly(butylene terephthalate), and the other part is properties of cyclic poly(butylene terephthalate)/ multiwalled carbon nanotube nanocomposites, including thermal behaviour of composites, mechanical properties of composites and the dispersion of multiwalled carbon nanotubes in composites.

It was found that the polymerisation and crystallisation of CBT occurs simultaneously and rapidly in a short time. The presence of multiwalled carbon nanotubes increases crystallinity of composites dramatically, but after adding MWNTs, the Young's modulus of the nanocomposites decreased. It is suggested that a crystalline structure makes the material less stiff. Although the fracture surface were not clearly under a scanning electron microscope, it is expected that carbon nanotubes dispersed homogenously at low weight percentage, but agglomerated when the proportion rose above 0.8wt%.

ACKNOWLEDGEMENTS

I would like to express my great appreciation to my supervisors, Dr. Stephen Kukureka and Dr. Mike Jenkins, for their patient guidance and useful advice for this research work. Without them, the project could not have been possible to finish.

I also deeply thank to Mr. Frank Biddlestone who always helped me solve a lot of technical difficulties in my experiments.

I would like to offer my special thanks to Professor David Book, Dr Isaac Chang, Professor Hanshan Dong and all staff from School of Metallurgy and Materials who have supported my study to go smoothly.

Finally, I wish to express my whole gratitude to my parents and my friends, in particular Qi Chen, Wenbo Dou, Qiongxi Liu and Yinghui Li, for their support and encouragement throughout my MRes study. They gave me an unforgettable experience in the UK.

CONTENTS

Chapter 1: Introduction

Chapter 2: Materials and Experimental Methods

LIST OF FIGURES

LIST OF TABLES

CHAPTER ONE

INTRODUCTION

1.1 Cyclic polyesters

Polyesters were one of the earliest families of polymers, and have played an important role in industry over the past decade. Cyclic polyesters have shown substantial differences between their linear analogues with unique properties when compared to their linear counterparts in processing. Rather than traditional polymers growing from a monomer into a long entangled, branching chain, cyclic polyesters grow from loop oligomers to a ring structure [1]. It is the loop shape with no end groups of cyclic polymer materials that give unique properties when compared to their linear counterparts. This involves direct change in physical and chemical behavior like increasing glass transition temperatures (T_g) and lower viscosities [2]. In addition, it also possesses some other unexpected properties which give rise to the application to a wider field. For instance, the change in biodistribution of cyclic polymers from the liner ones means that they might have advantages in novel drug delivery vector and thus is promising in biomedical industry [3].

Two kinds of polymerisation of cyclic oligomers, ring opening polymerisation (ROP) and ring expansion polymerization have been reported [4]. Cyclic catalysts lead to ring expansion polymerization while linear catalysts cause ring opening polymerization. For example, in this report, stannoxane, a cyclic catalyst, will be used to produce macrocyclic polymers.

One of the advantages of cyclic polymers is they have a low viscosity like water. The other advantage is that crystallization and polymerization start simultaneously, which do not require further cooling in demoulding. This drastically reduces the cost and time in

industry [5]. But the manufacturing industry is more interested in the low melt viscosity in order to blend the polymer with other materials producing composites.

1.2 Poly (butylene terephthalate) and its cyclic oligomers

The main limitation in fabricating continuous fiber thermoplastic composites is that fibers are hardly homogeneous dispersed in matrices due to the high viscosity of polymers [6]. In recent decades, cyclic butylene terephthalate (CBT) oligomers have been considered an advanced matrix material for composites. The low viscosity of the CBT, ability to be rapidly polymerized and crystallized, and no chemical emissions during processing make it easy to fill in thermoset polymers. CBT also exhibits the properties of thermoplastics such as higher toughness, better impact resistance and melt recyclability [7].

Cyclic butylene terephthalate is a cyclic oligomer which polymerizes to polybutyleneterephthalate (PBT) after adding a catalyst. Polymerisation of CBT was reported over the range 160 ℃ to 200 ℃ [8].

Polybutylene terephthalate (PBT) is a thermoplastic engineering polymer, which is prepared through polymer condensation reaction of 1, 4-butanediol with terephthalic acid. PBT is a semi crystalline polymer with crystallinity reported in the range 35%-45%. Generally, the crystalline melting temperature is from 225 ℃ to 232 ℃ and the typical glass transitiont emperature (T_g) is in the range from 30 to 50 ℃ [9].

The chemical structure of polybutylene terephthalate and cyclic PBT are shown in Figure 1.1 and 1.2 respectively.

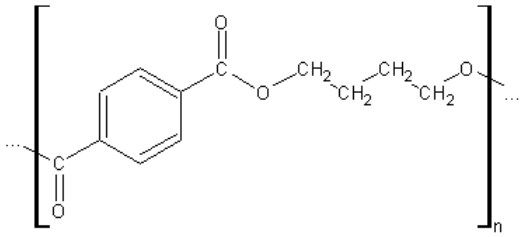

Figure 1.1: Chemical structure of linear PBT [8]

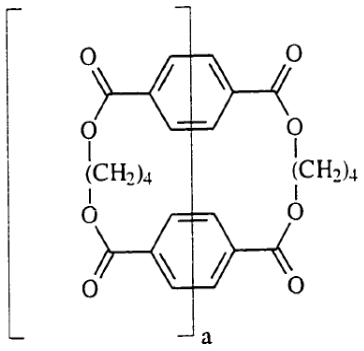

Cyclic PBT (a =1 - 6)

Figure 1.2: Chemical structure of cyclic PBT [8]

Baets [10] *et al*. added carbon nanotubes (CNTs) in CBT to improve ductility using VARTM (vacuum assisted RTM). The properties of samples were studied by three point bending, DSC and TEM. The results showed that carbon nanotubes increase the stiffness, strength and energy to failure, but decreases the failure strain slightly. In addition, the CNTs made no contribution on the crystallinity.

Romhany [11] *et al.* mixed pCBT and multi-walled carbon nanotubes (MWNT) using solid-phase high-energy ball milling (HEBM) for 10 min. After *in situ* polymerization, the crystallinity was calculated by Wide-angle X-ray scattering (WAXS) and DSC. According to the results, the crystallinity of c-PBT had no significant change. Moreover, mechanical properties were found that the filled CBT had a higher flexural modulus, strength, and impact strength. Finally, the ball milling had an active impact on carbon nanotube dispersion. The existence of an optimum concentration of MWNT was range from 0.25 wt% to 0.5 wt%.

Gabor Balogh [12] *et al*. mixed pCBT and graphene by hot pressing to make a nanocomposite. The graphene content ranged from 0.1 wt% to 5 wt%. DSC, DMA and TGA were used to analyze thermal properties. The results showed that graphene developed the pCBT crystallization and reinforced the pCBT matrix. But graphene had a poor dispersion in nanocomposite. There still remained clumps after *in situ* polymerisation.

Fabbri, Paola [13] also blended CBT and graphene by weight content 0.5, 0.75 and 1.0 wt% respectively. After *in situ* polymerization, CBT chains disperse homogeneously inside the interlamellar channels of graphene. The Young's modulus and Vickers Hardness increased for the content of graphene below 0.75wt%.

1.3 Polymerisation of CBT using stannoxane

Unlike the traditional step growth polymerisation of linear PBT, a cyclic oligomer CBT cannot open its ring structure by itself, so it must be reacted with a cyclic catalyst, 1,1,6,6-Tetrabutyl-1,6-di-stanna-2,5,7,10-tetraoxacyclodecane (stannoxane) (see Figure 1.3). The four Sn-O bonds in stannoxane are particularly active sites which not only allow ring expansion polymerisation but also remain in the cyclic structure of polymer [14].

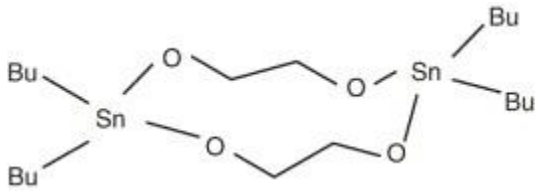

Figure 1.3: Structure of stannoxane catalyst [14]

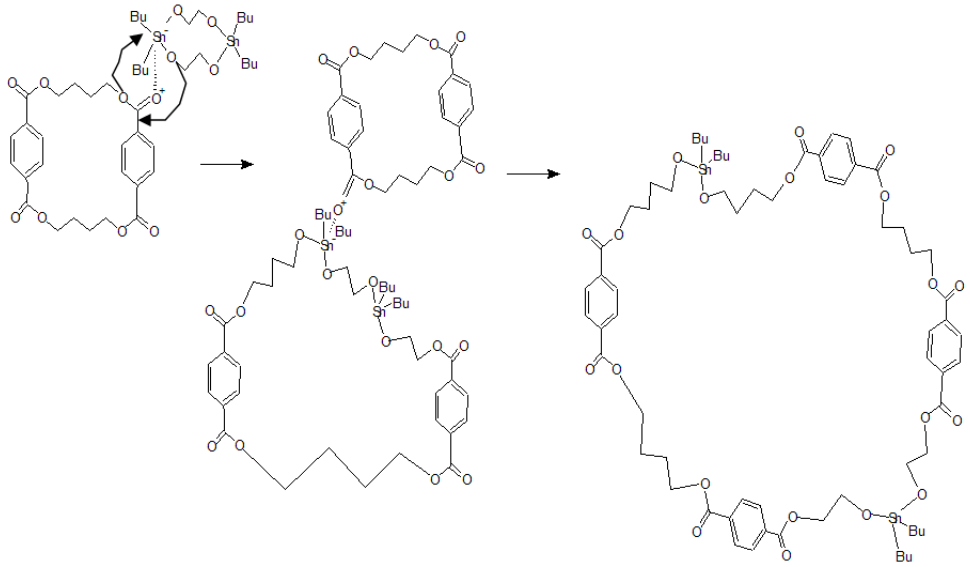

Figure 1.4: Ring growth mechanism of CBT with stannoxane catalyst [8]

Figure 1.4 illustrates the polymerisation mechanism that occurs between stannoxane and CBT. A bond exchange takes place which results in the breaking and reforming of one Sn-O bond in the stannoxane and one C-O bond in the ester group of the CBT. Stannoxane initiator inserts in the ring molecule so that increases the size of the ring. Once the first ring has been opened, other CBT molecules are still able to insert in stannoxane, attaching on the remaining three Sn-O bond [8]. However, this process does not produce polymerisation exotherm. As a consequence, the chain structure is large macrocyclic molecules incuding PBT repeat units and the stannoxane initiator. Because of the continuously ring expanding process, the molecular weight of cyclic PBT is higher than material produced by normal step polymerisation.

1.4 Carbon nanotubes

Carbon nanotubes (CNTs) are understood as a promising candidate as a reinforcing filler in nanocomposites. Nanotubes are allotropes of carbon and a member of the fullerene structural family. It is well known that CNTs has a cylindrical nanostructure with a high aspect ratio (about 132,000,000:1), and also has outstanding properties like thermal, mechanical, and electrical properties [15].

Carbon nanotube can be seen as a cylindrical tube rolled by a sheet of graphite, and each layer is composed of a hexagon carbon ring structure. According to the graphite layer, there are two types of carbon nanotubes: single-walled nanotubes (SWNTs) and multi-walled nanotubes (MWNTs) [16].

Carbon nanotubes can be made by chemical vapor deposition, carbon arc methods, or laser evaporation. They are capable as additives in various fields such as nanotechnology, electronics and structural materials [17].

The majority of carbon atoms in carbon nanotubes are with sp^2 hybridization. Since the hexagonal structure bending in three-dimensional space, some of the carbon atoms form a sp^3 hybridization. Thus the formation of chemical bonds is sp^2 and sp^3 hybridization state at the same time [18].

In addition, carbon nanotubes are not always straight cylinders. Sometimes convex and concave are constitutes of pentagon and heptagon. If the pentagon appears at the top of the carbon nanotubes, carbon nanotubes will be sealed. When a heptagon appears in nanotubes, carbon nanotubes will be dented. These morphology defects can change the structure of carbon nanotubes, while the structure of electronic band near the defect will also change.

The atomic structure of nanotubes is described by the chiral vector, $\vec{C}_h$, and the chiral angle, θ (Figure 1.5). The chiral vector, often known as the roll-up vector, can be described by the following equation [19]:

$$\vec{C}_h = n\vec{d}_1 + m\vec{d}_2$$

where the integers (n, m) are the number of steps along the ziz-zag carbon bonds of the hexagonal lattice and $\vec{d}_1$ and $\vec{d}_2$ are unit vectors.

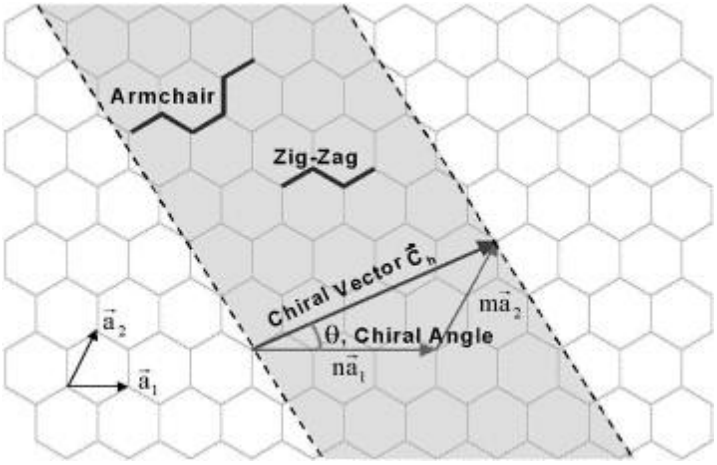

Figure 1.5: Schematic diagram showing how a hexagonal sheet of graphite is 'rolled' to form a carbon nanotube [19]

When n = m, called armchair carbon nanotubes and chiral angle is 30 °. When n > m = 0, called the zigzag carbon nanotubes and chiral angle is 0 °. When n > m ≠ 0, called chiral carbon nanotubes [19].

Fig. 1.6 shows the structures of armchair (n, n) and zig-zag(n, 0) nanotube is in terms of the roll-up vector.

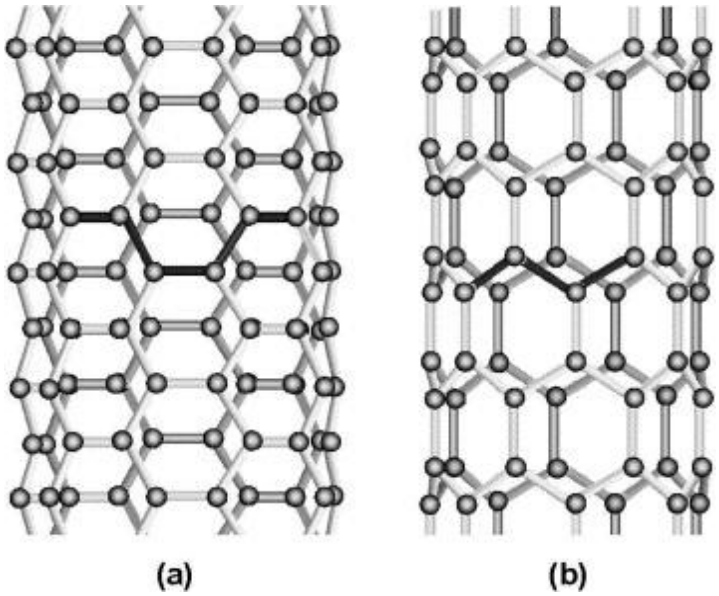

Figure 1.6: Illustrations of the atomic structure of (a) an armchair and (b) a ziz-zag nanotube[19]

It is reported that carbon nanotubes have a very high stiffness and strength. They have elastic modulus as high as 1.0 TPa while steel is approximately 0.2 TPa and tensile strength in the range of 10–50 GPa while steel is 0.25GPa [20]. The extremely high Young's Modulus is because the chemical bonding of carbon nanotubes, sp^2 carbon–carbon bonds. This structure provides carbon nanotubes with extremely high mechanical properties.

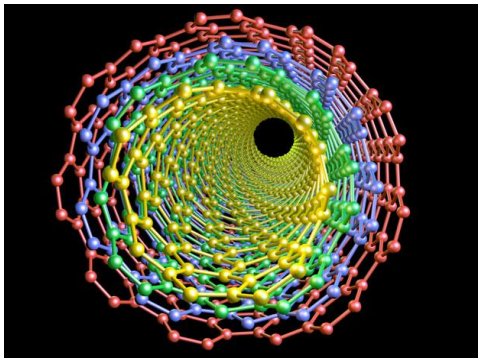

Figure 1.7: Multi-walled carbon nanotubes [21]

Previous researches have studied blending carbon nanotubes with different polymers, e.g. PVF [22], PE [23] and PMMA [24]. However, the biggest challenge is the cluster or agglomerate of nanotubes because of the strong van der Waals forces between each tube. As a consequence, the CNTs are difficult to disperse homogeneously in polymer matrix.

Wu [25] *et al.* prepared samples with different content of MWNT(1-7wt%) by melt mixing in a Rheometer. The nucleation effect of MWNT and nonisothermal crystallization process were obtained by XRD and DSC. The results revealed that MWNTs worked as an efficient nucleation and leaded to a higher crystallinity of PBT. However, they might cause reduction of polymer chains mobility to some extent. Besides, the MWNT nearly did not influence the thermal stability of PBT matrix.

Wu [26] mixed PBT containing dibutyl tin(IV) oxide and hydroxyl-functionalized multiwalled carbon nanotubes before the ring open polymerization. The dispersion state was carried out by the FESEM and TEM. The results indicated when the proportion of MWNTs was less than 0.75 wt%, it could be seen MWNTs dispersed homogeneously in the PBT matrix. Moreover, the DSC results showed that the presence of MWNTs was regarded as a good nucleation and accelerated the crystallization rate of PBT. And MWNTs also had a contribution on the thermalstability of composite.

1.5 Preparation of carbon nanotube/ polymer composite

Polymer blends can be miscible, immiscible or partially miscible depending on physical and chemical interactions between the chains of the constituent homopolymers.

Due to $\Delta G = \Delta H - T\Delta S$ [27],

where ΔG is change in free energy, ΔH is change in enthalpy, ΔS is change in entropy and T is temperature.

For small molecules or atoms, ΔH is positive and ΔS is hugely positive, so ΔG is negative. The result is small molecules or atoms can be mixed. On the other hand, for polymers, ΔH is positive and ΔS is slightly positive, so ΔG is positive as well. The result is polymers do not mix.

Besides, because of the heavily agglomerate of carbon nanotubes, dispersion of CNTs and poor interfacial interaction between CNTs and polymer matrix are the biggest difficulties during processing.

1.5.1 Solution mixing

Solution mixing is the simplest method for preparing carbon nanotube/ polymer composite. The main steps of this method involve mixing CNTs in a polymer solvent at suitable temperatures and then evaporating the solvents [28]. Before mixing nanotubes are usually functionalized first. The shortage of solution mixing is the entanglement of carbon nanotubes, leading to inhomogeneous dispersion of nanotubes in matrix. This method is often used to prepare composite films.

1.5.2 Ultrasonication

Ultrasonication is an effective method to disperse CNTs in low viscosity liquids, such as water, acetone and ethanol. In the laboratory, it is usually using an ultrasonic bath or an ultrasonic probe to disperse nanoparticles dispersion [29]. However, most polymers require to be dissolved or diluted in a solvent to reduce the viscosity before dispersion of CNTs. If the sonication treatment is too long, CNTs can be easily and seriously damaged.

1.5.3 Ball milling

'Ball mill is a type of grinding method used to grind materials into extremely fine powder for use in paints, pyrotechnics and ceramics' [30]. The principle of this technique is that balls and materials in a sealed container, the friction and collision between them grind materials to powder. The balls can be in different size and materials. The advantage of ball milling is that it is solvent free. It not only increases the dispersion of carbon nanotubes but also enhances the surface area of the materials hugely.

It is reported that the ball milling is considered to be an efficient way to improve the functionality and performance of carbon nanotubes. The length of the carbon nanotubes becomes shorter after ball milling. The short tubes can still act as a reinforcement like long tubes [31].

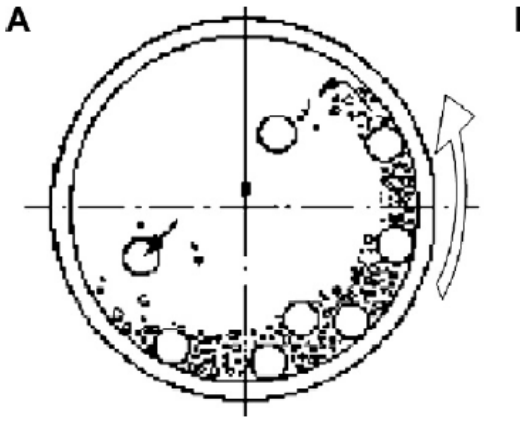

Figure 1.8: Ball milling [30]

1.5.4 Melt processing

Melt processing is often used in thermoplastic polymers. Solution mixing is limited to polymers dissolved in a common solvent. Melt processing is a alternative way to melt polymers when heated and then then mix with nanotubes. Due to the high viscosity of most polymers, it is hard to disperse carbon nanotubes homogeneously.

Hailian Wang [32] use a co-rotating twin-screw extruder to blend PE with CNTs ranging from 0.5 wt% to 12 wt% at different temperatures. It is observed the CNTs dispersed into PE in the forms of single nanotube, nanotube network, or aggregates. The electrical conductivity and thermal properties of composite were modified successfully. Furthermore, the addition of CNTs caused better thermal stability of the composite comparing with neat PE nanofibers.

1.5.5. *In situ* polymerization

The traditional way producing carbon nanotube/ polymer composite is melt processing. An alternative method is called *in situ* polymerization. It is an efficient method to disperse CNTs in a thermosetting polymer.

In this method, polymers do not need prior melting. CNTs are mixed with monomers directly in the presence or absence of a solvent. Then these monomers are polymerized with catalyst. The advantage of this method is the higher mechanical properties of

composites because of strong interfacial bonds formed between the CNTs and polymer matrix [33].

1.6 Carbon nanotubes with other matrix

There are also large amount of reports of carbon nanotubes with other matrixes, such as metal and ceramic.

Chih-Wei Chang [34] used differential scanning calorimetry (DSC) to analyze thermal decomposition and thermodynamic of CNT/ Al_2O_3 composite. It is showed that the thermal delay effect increased the exothermic onset temperature and decreased the heat decomposition of composite. In addition, the composite is safer than activated carbon and CBT. Lastly, the exothermic reaction was first order for composite and had the activation energy increase as the heating rate increased. MWNT in composite would have much lower heat of decomposition than MWNT in commercial CNT.

Anastasia Sobolkin *et al.* [35] mixed cement paste with carbon nanotubes by aqueous dispersions. To improve the dispersion of CNTs, sonication in combination with anionic and nonionic surfactants was used. For hardened cement paste modified with the CNTs, the compressive strength increased dramatically but the strength had no significant improvement.

1.7 Aims and objectives

Since CBT has a low molecular weight and melt viscosity, it is a very promising material for composites, but the pure CBT is brittle. The high stiffness of carbon nanotubes makes it as an excellent candidate for filler materials. So CBT and CNTs are chosen to blend a composite in this study.

The composites were prepared by a novel method called *in situ* polymerisation. The main advantage of this method is that CBT is polymerised inside the blend system and polymer macromolecules are able to graft onto the walls of carbon nanotubes. Furthermore, this technique is particularly important for the preparation of insoluble and thermally unstable polymers which cannot be processed by solution or melt processing [36].

Nowadays extrusion molding or injection molding are widely applied in polymer processing. These methods melt polymer granules first, and polymerization occurs during the mixing process. Solid dispersion does not need heat polymer at a particular temperature and it mixes blend components before polymerisation. So the solid dispersion which prevents premature phase separation and allows homogeneous phase dispersion is prior to extrusion molding or injection molding [37].

This study focused on the thermal behaviour of CBT and the properties of cyclic PBT/ Multi-walled carbon nanotube composite. The thermal behaviour of CBT, simultaneous polymerisation and crystallisation, and the thermal behaviour of composites were studied by Differential Scanning Calorimetry (DSC). Functional groups in CBT and in situ polymerisation effect on functional groups of CBT were investigated by Fourier Transform Infrared Spectroscopy (FTIR). Mechanical properties of CBT and composites were tested by nanoindentation. The dispersion state (miscible or immiscible) of CBT/ MWNT composites was observed by Raman spectroscopy and scanning electron microscope (SEM).

CHAPTER TWO

MATERIALS AND EXPERIMENTAL METHODS

2.1 Materials

2.1.1 Cyclic butylene terephthalate oligomers (CBT)

The CBT 160 was purchased from Cyclics Corporation (2135, Technology Drive, Schenectady, New York 12308, USA) in pellet form. The catalyst has been premixed with the resin which can be converted into the engineering thermoplastic polymer PBT [38].

The CBT used in this project was dried in a vacuum oven at 90 ℃ overnight before processing to remove residual moisture.

2.1.2 Multi-walled carbon nanotubes (MWNTs)

The CNTs (Multi Walled Nanotubes-MWNTs 95 wt% 10-20 nm OD) were provided by Cheap Tubes (3992 Rte 121 East, Cambridgeport, VT 05141 USA). The general properties from the manufacturer are shown in Table 2.1.

Table 2.1: The data sheet of Multi Walled Nanotubes-MWNTs 95wt% 10-20nm OD [39].

Outer Diameter	10-20 nm
Inside Diameter	3-5 nm
Length	10-30 um

Purity	>95 wt%
Density	2.1 g/cm^3(at 20℃)
Specific Surface Area	233 m^2/g
Electrical Conductivity	>100 S/cm
Forms	powder

2.2 Experimental methods

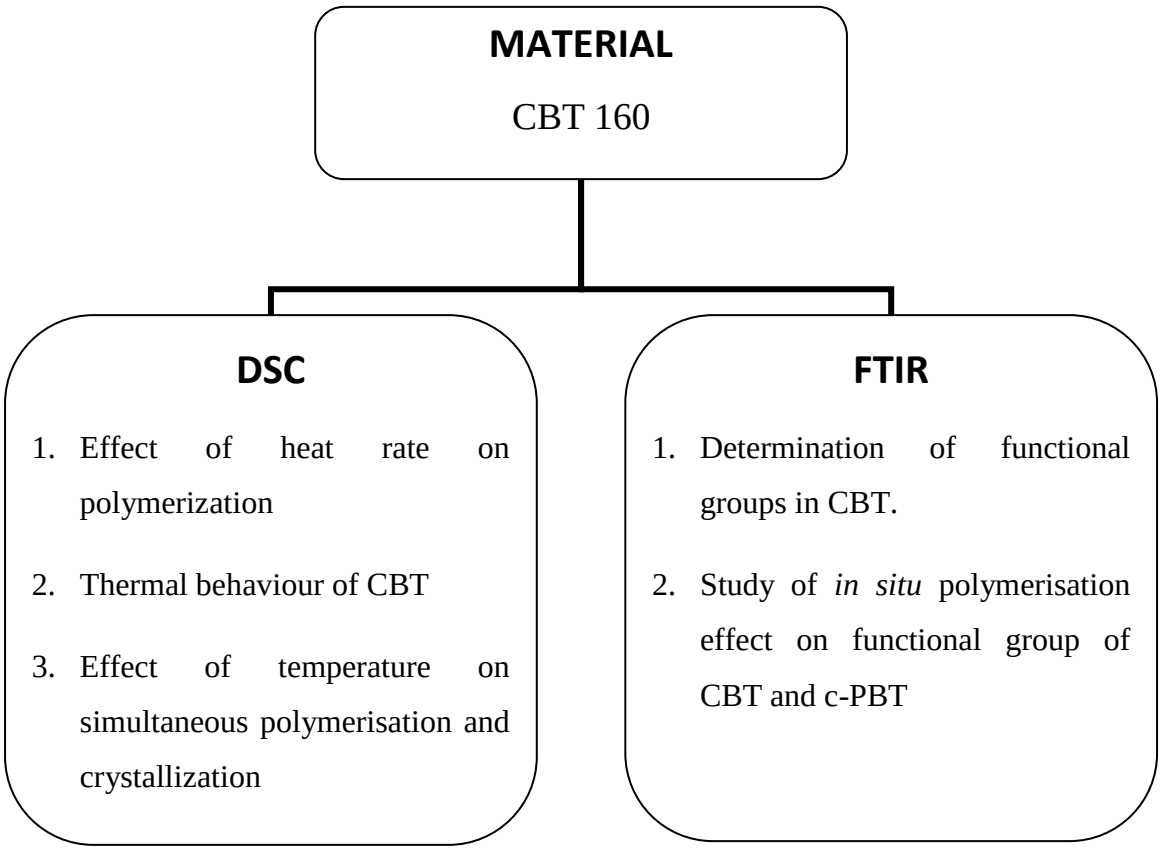

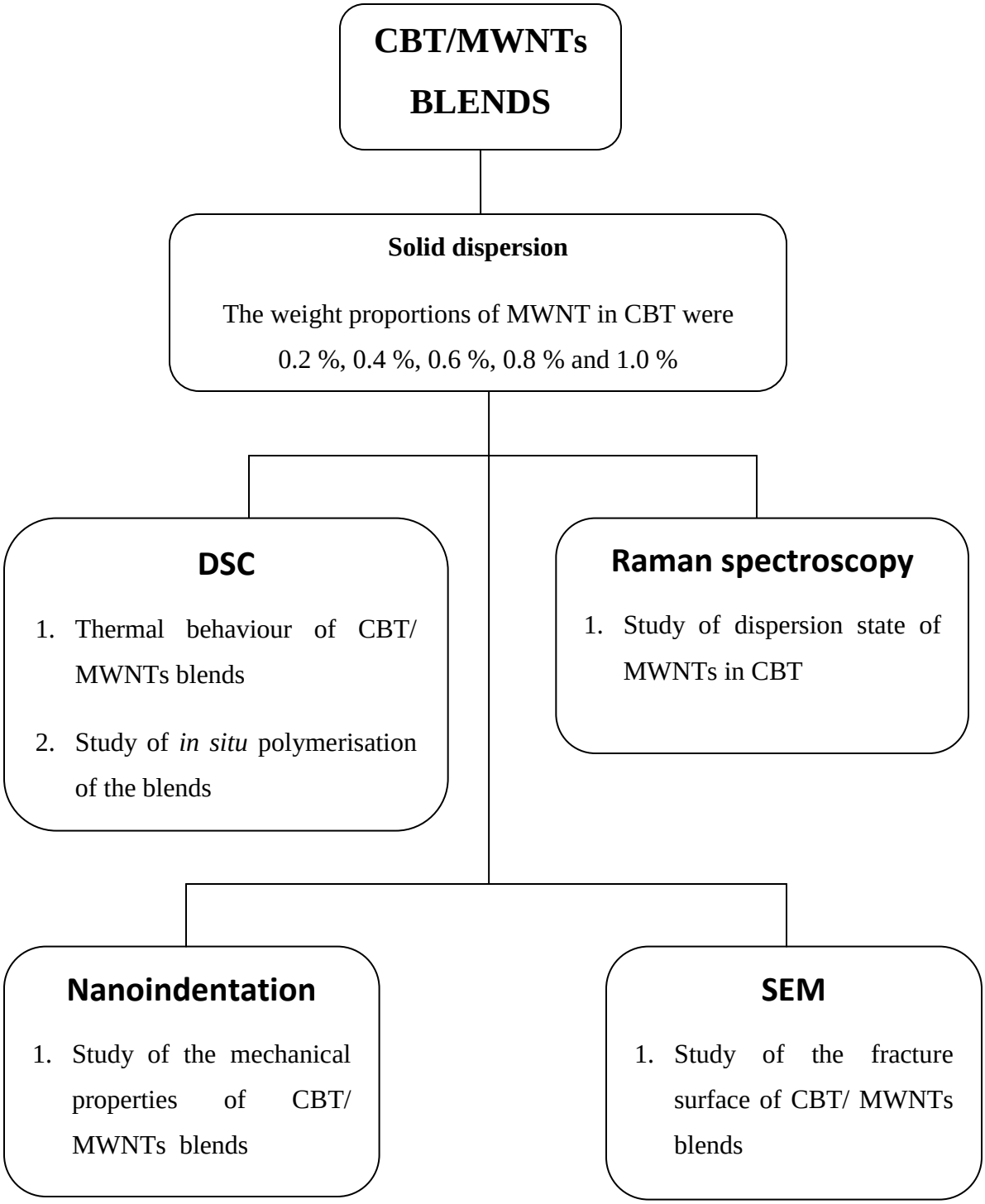

2.2.1 Sample preparation

The dried CBT and MWNT powder were blended in various proportions using a Pulverisette 5 Planetary Ball Mill Glen Creston (London, UK). The apparatus is shown in figures 2.1 and 2.2. The diameter of stainless steel jars D_j is 25 mm and the depth of stainless steel jars d_j is 85 mm. The diameter of stainless steel ball D_b=10 mm and the weight of each ball m_b is 4 g.

According to previous studies [10, 25, 26], the optimum properties of composites were found in the MWCNT range of 0.1 – 1.0 wt%. So in this study, the weight proportions of CBT/MWNT used were 0.2 %, 0.4 %, 0.6 %, 0.8 % and 1.0 %. According to Romhany's study [11], the mass ratio of the stainless steel balls to sample was 5:1 and the speed for ball mill was 200 rpm. The time of mixing was decided to be 3 min, 5 min, and 10 min. When the ball milling lasted 3min, the CBT and MWNT do not mix very well because some white granule, the CBT, still existed after ball milling. Due to the heat produced during ball milling, the samples milled for 10min are polymerised. So the time of ball milling of the CBT/ MWCNT was chosen at 5 min to prevent the temperature not becoming too high so that the polymer does not polymerise prematurely.

Figure 2.1: Pulverisette 5 Planetary Ball Mill Glen Creston

Figure 2.2: Stainless steel jar and balls

2.2.2 Differential Scanning Calorimetry (DSC)

2.2.2.1 Introduction

Differential scanning calorimetry is one of the techniques that can be used to analyse both qualitative and quantitative thermal information about physical and chemical changes in materials. DSC is used widely for examining polymeric materials to determine their thermal transitions, such as the glass transition, crystallisation point, degree of crystallinity, melting point, thermal degradation and heat of fusion [40]. One of the advantages of DSC is examining materials using only a small amount of material.

The basic principle of differential scanning calorimetry is when samples undergo a transition (e.g. the glass transition or a chemical reaction), they will absorb or release heat. The sensors and heaters keep the sample and the reference at the same temperature and measure the endothermic or exothermic heat difference between the specimen and the reference [41].

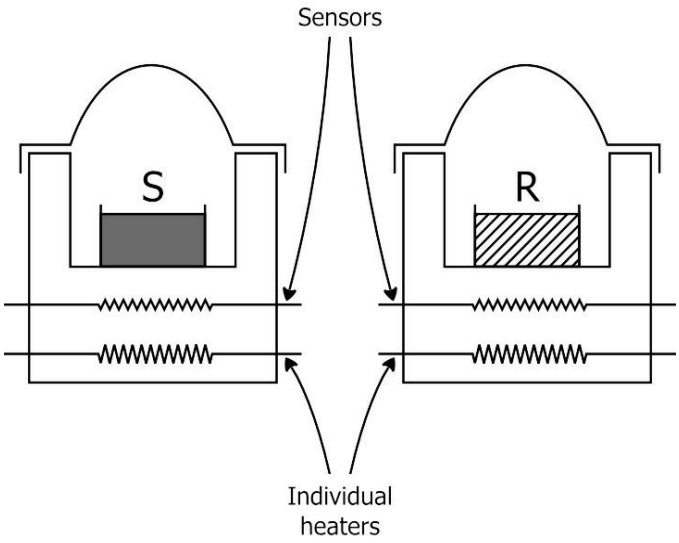

Figure 2.3: Basic principle of DSC [8]

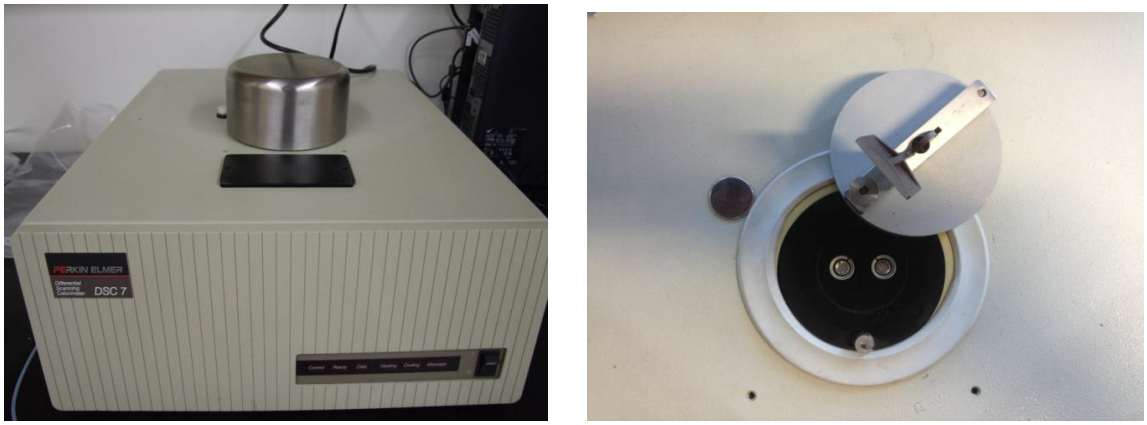

Figure 2.4: Perkin–Elmer differential scanning calorimeter (DSC-7)

In this study, the thermal analysis of the materials used a Perkin–Elmer differential scanning calorimeter (DSC-7) (Figure 2.4). This machine contains of two chambers. The reference pan is often an empty pan. The software for data analysis is Pyris Manager.

To study the thermal behaviour of CBT and composites, every sample was 15 mg, weighed to 0.5 mg on a microbalance. The same aluminum pans and lids were used for all samples. The DSC was calibrated by Indium and Sn respectively.

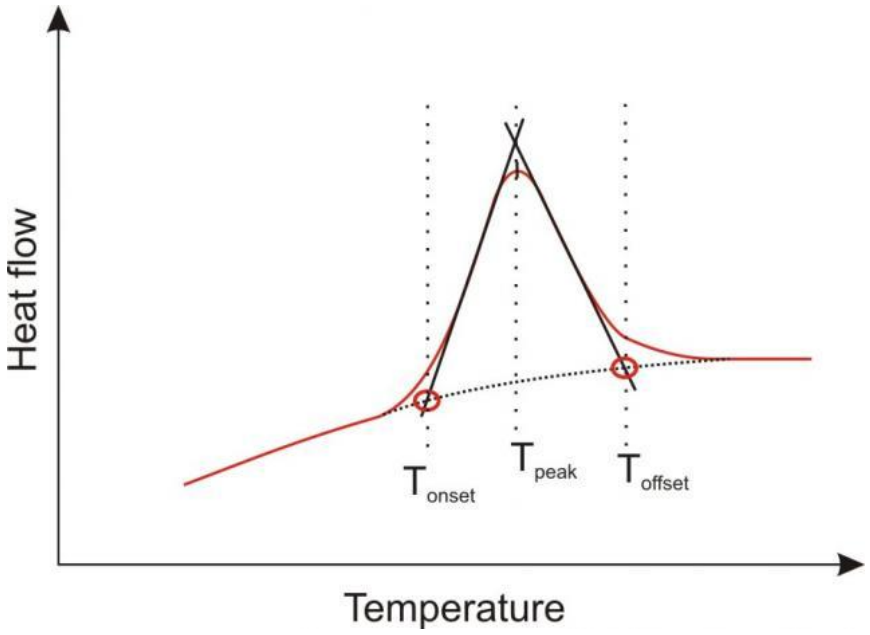

Figure 2.5: The typical melting transition of semi-crystalline polymer [42]

Figure 2.5 showed the melting transition of semi-crystalline polymers. The melting temperature of polymer is not a fixed temperature. It ranges from onset temperature to offset temperature [42].

In a DSC curve shown above, the area under a melting transition curve is the total amount of heat absorbed (ΔH_m) during the melting process. The degree of crystallinity (X_c) for the PBT and PBT/MWNT nanocomposites was calculated from the enthalpy evolved during crystallization on the basis of the cooling scans with the following equation [5]:

$$X_c\ (\%) = (\Delta H_m/\Delta H_o) \times 100$$

where ΔH_m is the measured heat of fusion for the sample and ΔH_o is the heat of fusion of a 100% crystalline polymer. According to previous studies, the heat of fusion of 100% crystalline PBT is 140 J/g [5].

2.2.2.2 Effect of heat rate on polymerisation

In order to understand how the heat rate influenced the polymerisation, the sample was heated from room temperature to 240 ℃ at different rates: 10 ℃/min and 5 ℃/min.

2.2.2.3 DSC dynamic scan of materials

To study the thermal behaviour of materials, first, heated the sample from 25 ℃ to 250℃ at a rate of 5 ℃/min. Second, the sample was held at 250 ℃ for 2 min. Third, cooled back the sample to 25 ℃ at 10 ℃/min cooling rate. Fourth, the same sample was heated again to 250 ℃ and then cooled back to room temperature at a rate of 10 ℃/min.

2.2.2.4 Effect of temperature on simultaneous polymerisation and crystallisation

To study the simultaneous crystallisation and polymerisationof CBT, first, the sample was heated to the target temperature quickly, for example, target temperature in 170 ℃, 180 ℃, 190 ℃, 210 ℃ and 220 ℃. Second, held the sample at the target temperature for 60 min and cooled back to room temperature. Third, reheated the same sample to 250 ℃ at 10 ℃/min and then cooled back with the same rate. Finally, the last step was repeated to record results.

2.2.2.5 *In situ* polymerisation of the composites

According to Samsudin [8], the optimum condition to produce c-PBT was found to be 190 ℃. The samples were heated with composition of CNTs in the range from 0.2 wt% to 1.0 wt% from room temperature to 190 ℃ rapidly (160 ℃/min), and then held at the target temperature for 60 minutes. After that they were cooled back to 30 ℃. The same sample was reheated to 250 ℃ at 10 ℃/min and then cooled back with the same rate.

2.3 Fourier Transform Infrared Spectroscopy (FTIR)

2.3.1 Introduction

All the atoms which form chemical bonds or functional group vibrate constantly, so when we use infrared radiation in a sample, different molecular structures will create a unique fingerprint. Infrared spectrometry is a method of analyzing the information of vibration and rotation between the atoms to determine the molecular structure and compounds of materials. A basic IR spectrum is a graph that wavelength on the horizontal axis shows

absorption peak position and infrared light absorbance (or transmittance) on the vertical axis shows absorption intensity [43].

Fourier transform infrared (FTIR) spectrometer is a rapid and non-destructive technique widely used in laboratories to exam the functional group. The advantage of FTIR is that the sample can be solid, liquid, or gaseous [44]. The infrared spectrum is usually divided into three regions, the near- infrared (approximately 14000 – 4000 cm^{-1}), the mid-infrared (approximately 4000 – 400 cm^{-1}) and far- infrared (approximately 400 –10 cm^{-1}) [45].

In this study, FTIR spectra were obtained on Nicolet Magna IR-860 FTIR spectrometer. All spectra were recorded from 400-4000 cm^{-1}. A total of 100 scans at a resolution of 2 cm^{-1} were averaged.

2.3.2.2 Study of in situ polymerisation effect on functional group of CBT and c-PBT

To study the effect of in situ polymerisation on functional groups of the CBT, a sample of CBT on a potassium bromide (KBr) disc was placed on the hot-stage sample holder. This hot-stage was connected to the Nicolet Magna IR-860 FTIR spectrometer to measure FTIR spectra using transmission technique. A background absorption spectrum was taken at room temperature before heating the sample. Then the hot-stage was heated from 100 ℃ to 240 ℃ at every 10 ℃ interval.

2.2.4 Raman spectroscopy

2.2.4.1 Introduction

When a laser beam illuminates a sample, an electron is excited from the valence energy band to the conduction energy band by absorbing a photon. The excited electron is scattered by emitting (or absorbing) phonons, and the electron relaxes to the valence band by emitting a photon. Elastic scattering is the wavelength of scattering light as same as the laser, while inelastic scattering is the wavelength of scattering light different from the laser and it known as the Raman scattering. The laser light interacts with molecular vibrations, phonons or other excitations in the system, resulting in the energy of the laser photons being shifted up or down [46].

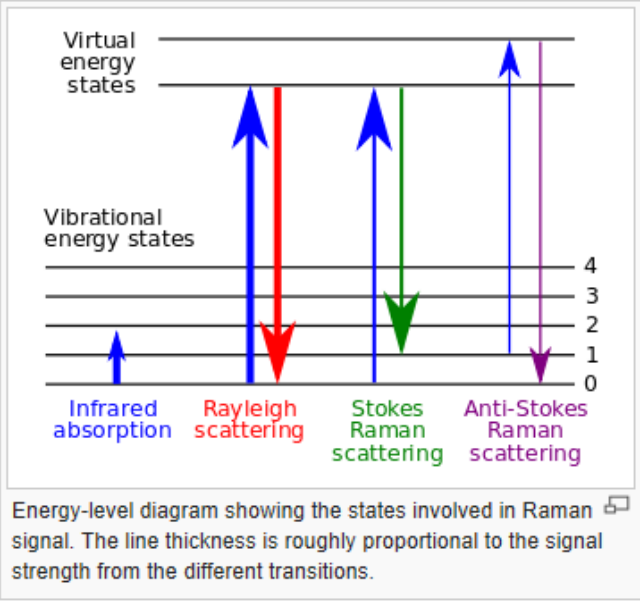

Figure 2.6: Basic principle of Raman spectroscopy [47]

Raman spectroscopy is a technology which provides a quick, simple, repeatable, and non-destructive testing for materials. In Raman spectrum of carbon nanotubes, there are usually two strong peaks called G band and D band. G band is around 1582 cm^{-1} and the D band is around 1350 cm^{-1}. The D band originates from a hybridized vibrational mode and it indicates the presence of some disorder in structure. The G band is often used as a measure of the quality of the nanotubes [48].

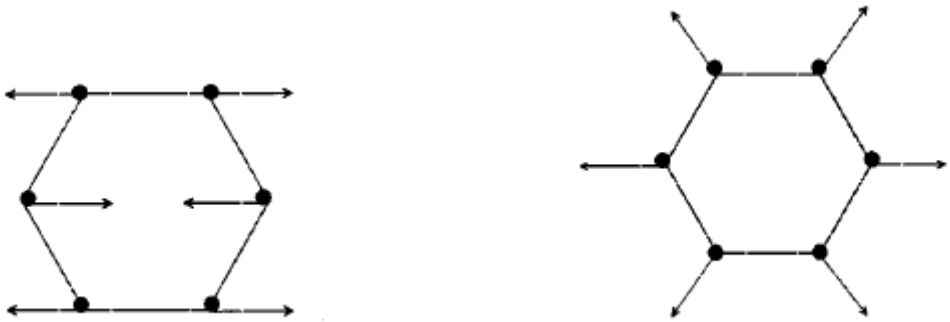

(a) (b)

Figure 2.7: Carbon motions in the G band (a) and D band (b) [49]

2.2.3.2 Raman spectroscopy experimental procedures

In this study, the samples were prepared by DSC. 15mg samples were weighed in the DSC pan and kept at 190 ℃ for 1 hour. After that I quenched the pan into liquid nitrogen and extract the sample from the DSC pans.

To investigate whether multiwalled carbon nanotubes disperse homogenously in CBT, all Raman spectra were recorded by Renishaw InVia Reflex Raman Spectrometer with a 633nm laser. The software for data analysis is Renishaw Wire 3.4.

2.2.4 Nanoindentation

The three point bending was initially tried to examine the mechanical properties of composite. The samples were prepared using a hot press, but the material is too brittle. The sample was broken into pieces and cannot reach the size require for testing, so the nanoindentation was used as an alternative. The advantage of nanoindentation testing is that it can be used to measure the mechanical properties of materials on a micro-scale or even nano-scale.

2.2.4.1 Introduction

Nanoindentation was used to sensitively evaluate the hardness and Young's modulus. The traditional measurement is using a tip whose mechanical properties are known (frequently made of a very hard material like diamond) to press into a sample whose properties are unknown. The hardness H is defined as [50]

$$H = P_{max} / A_r$$

where P_{max} is the maximum load and A_r is the residual indentation area.

The disadvantage of this method is that it able to get the plastic property of material and it also need a large size sample. With the development of nanoindentation, now nanoindentation has been applied widely in mechanical testing of materials. It also can measure the hardness of small volumes of material [51].

2.2.4.2 Nanoindentation experimental procedures

In this study, mechanical properties were tested using a NanoTest 600 Platform 3 machine (MicroMaterial, UK). The samples were also prepared by DSC. To produce reliable results, each sample used the maximum load of 5mN repeated 5 times. The test rate was 1mN/s and then it was held for 10s. The resolution ensures 20nN on the loading system and 0.04nm on depth.

2.2.5 Scanning Electron Microscopy (SEM)

2.2.5.1 Introduction

The scanning electron microscope (SEM) is a method to identify the morphology on surface of materials. When a focused beam of electrons scans on the sample, it stimulates various signals on the surface of samples, including secondary electrons (SE), back-scattered electrons (BSE), characteristic X-rays, light cathodoluminescence (CL), specimen current and transmitted electrons [52]. The secondary electron detector is most common mode for all SEMs. The detector captures the secondary electron which is related to of the beam of light, so the image gives the topography of the sample.

2.2.5.2 SEM experimental procedures

To study the dispersion of multiwalled carbon nanotubes in CBT, the samples were prepared by DSC. 15 mg samples were weighed in the DSC pan and kept at 190 ℃ for 1 hour. After that the pan was put into liquid nitrogen and samples were extracted from the DSC pans. The fracture surfaces of the samples then were gold coated before photos were taken. The scanning electron microscopy (SEM) in this study was a Jeol 7000F (JEOL Ltd. Japan).

CHAPTER THREE

RESULTS AND DISCUSSION

3.1 DSC examination

3.1.1 Effect of heating rate on polymerisation

Figure 3.1 illustrates the heating trace of CBT at different rates, i.e. 5 ℃/min and 10 ℃/min.

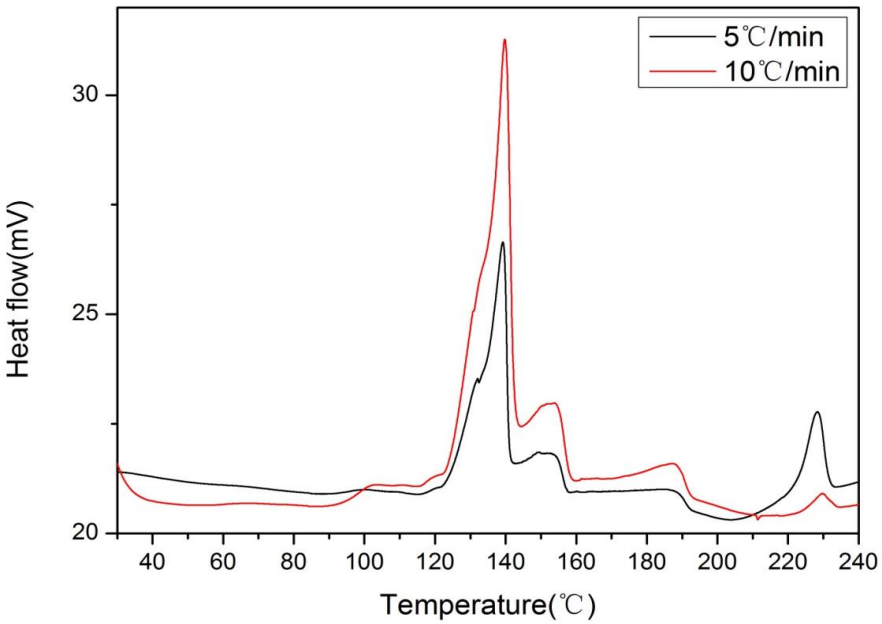

Figure 3.1: CBT at different heating rate

The melting peak of the oligomer (the peak at 130 ℃) at 10 ℃/min is bigger than that at 5 ℃/min due to the fast heating rate. On the other hand, the melting peak of polymer (the peak at 230 ℃) at 10 ℃/min less than the 5℃/min, because that more time is spent in the polymerisation region.

3.1.2 Thermal behaviour of CBT and c-PBT

Figure 3.2 illustrates the heating trace of CBT with catalyst at a rate of 5 ℃/min.

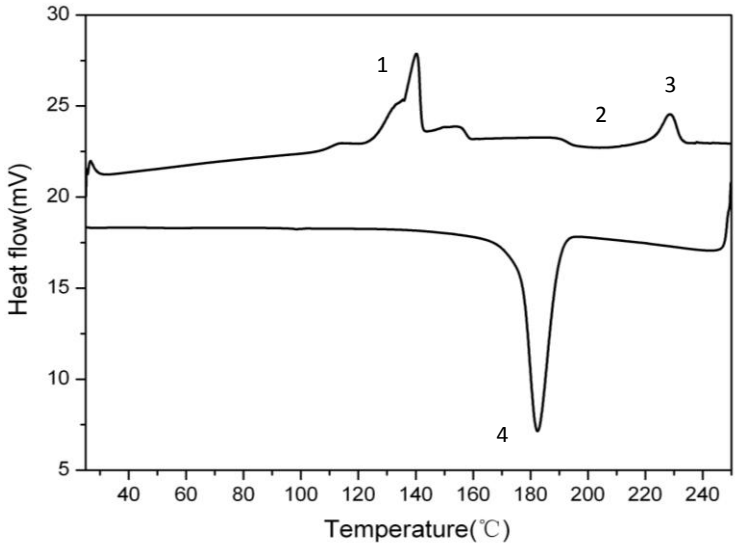

Figure 3.2: Typical DSC heating and cooling trace of CBT

The initial DSC scan of CBT reveals the temperatures of oligomer melting (1), polymerisation and crystallisation (2), polymer melting (3) and re-crystallisation (4). From Figure 3.2, it can be seen that CBT is found to melt over a broad range. The oligomer melting occurs at 120 ℃ -160 ℃. At this temperature, the CBT changes from solid phase to low viscosity liquid. There are several peaks which mean different kind of oligomers melting. In addition, simultaneous polymerisation and crystallisation processes start at approximately 168 ℃ and finish at about 216 ℃. After the *in situ* polymerization, the c-PBT continually melts at 229 ℃. Finally, during cooling, an exothermic dip has appeared at 183 ℃; this is indicated to be the polymer re-crystallisation, since the polymerisation is an entropically driven ring-expansion polymerisation, resulting in an almost thermoneutral reaction.

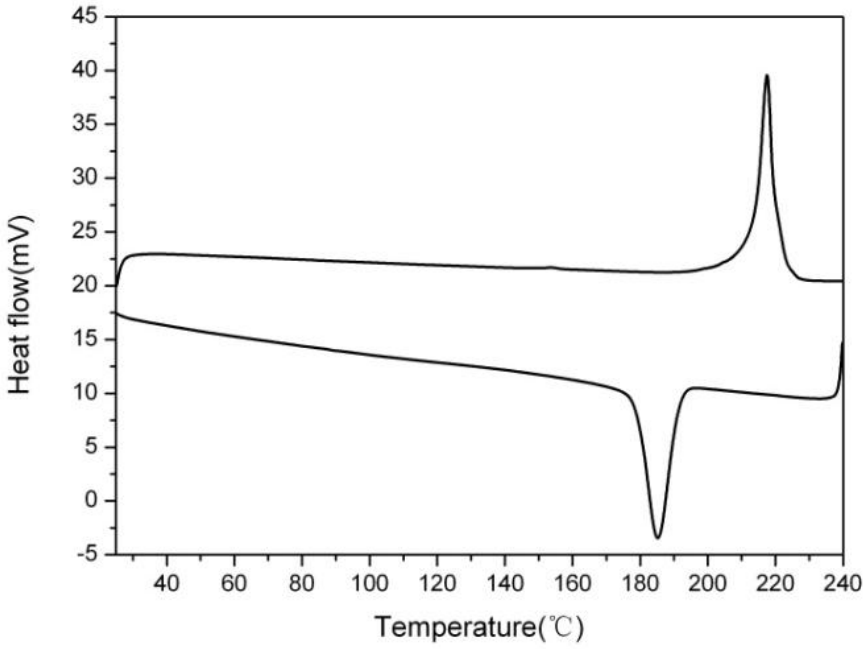

Figure 3.3: Typical DSC re-heating of c-PBT

From Figure 3.3, it is obvious that there is no oligomer melting peak in the second dynamic run of the c-PBT, so it appears that all the oligomer converts to polymer in the first dynamic run. The polymer melting peak is observed higher than that in first dynamic run. This situation is believed to be due to high degrees of crystallisation after melting and re-crystallisation.

From previous studies [10-12], it is concluded that the active temperature for the ring expansion polymerisation could begin at 160 ℃. It is known that the *in situ* polymerisation of CBT occurs simultaneously with the crystallisation process. Since the melting point of the CBT is below that of c-PBT and the conversion from CBT to c-PBT is sufficiently rapid at relatively low temperatures, isothermal processing below the melting point of PBT is possible. Depending on the degree of supercooling and the reaction speed, this isothermal processing may result in simultaneous polymerisation and crystallisation. However, with thermal analysis techniques such as DSC, only the crystallisation process could be monitored since the cyclic oligomers are nearly strain-

free which means their polymerisation is almost thermo-neutral. It is also believed that CBT must be converted to a polymer of sufficiently high molecular weight before crystallisation can commence.

Figure 3.4 shows the crystallisation process of CBT in this temperature range 170 ℃ to 220 ℃.

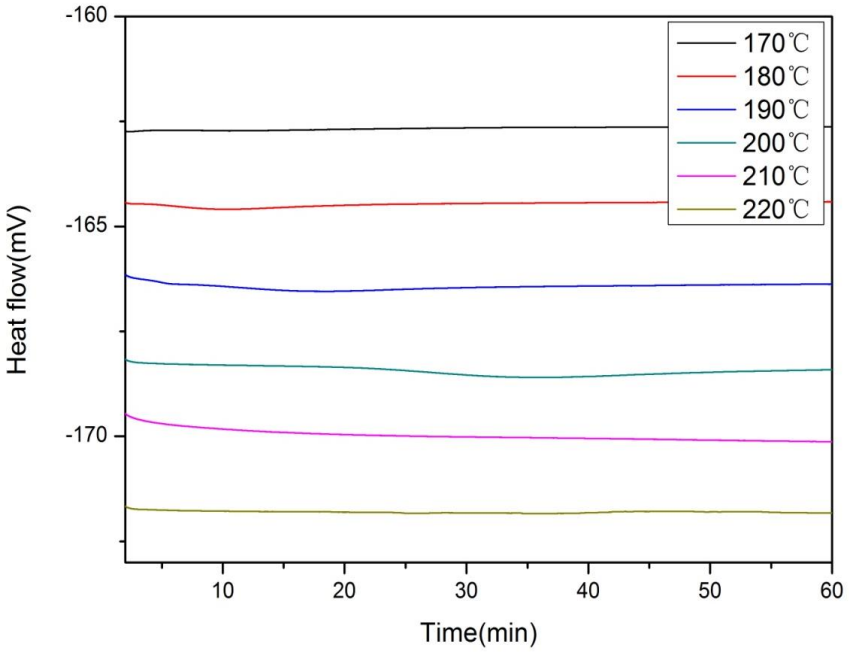

Figure 3.4: Simultaneous polymerisation and crystallisation of CBT at various temperatures

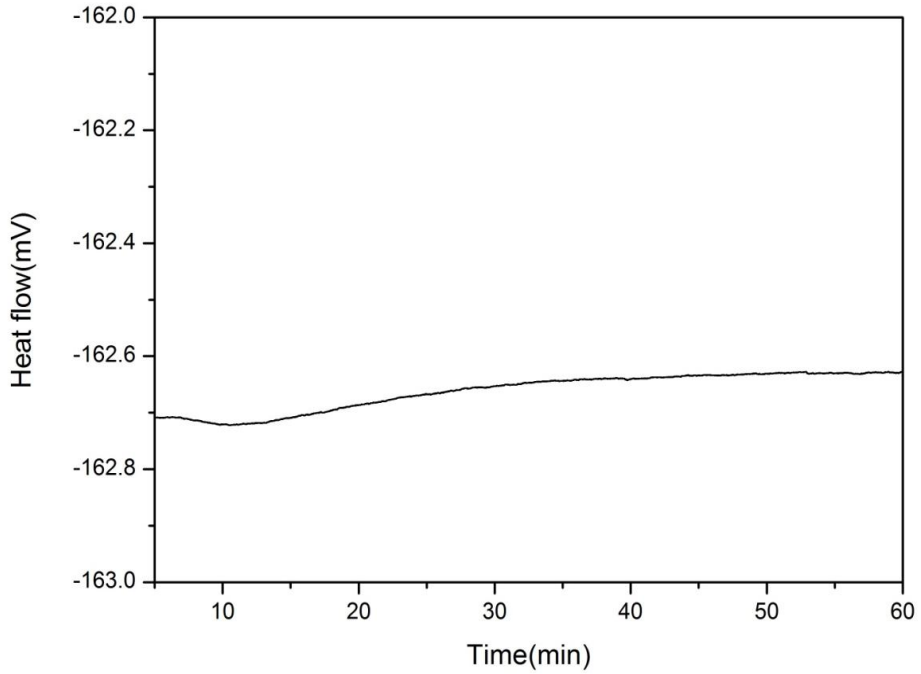

Figure 3.4.1: Simultaneous polymerisation and crystallisation of CBT at 170 ℃

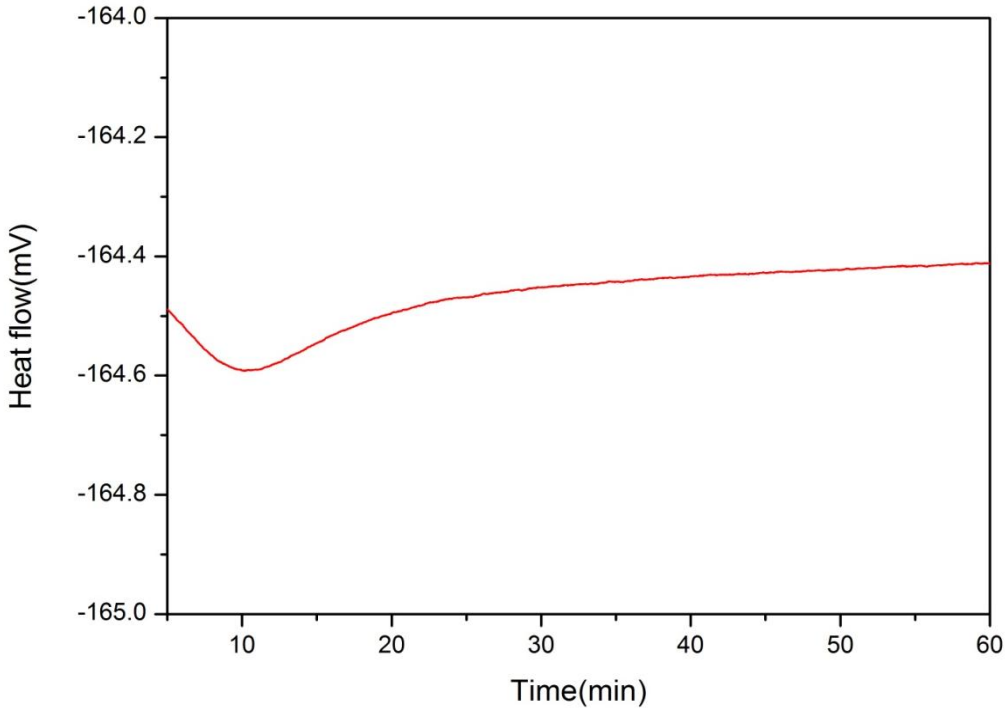

Figure 3.4.2: Simultaneous polymerisation and crystallisation of CBT at 180 ℃

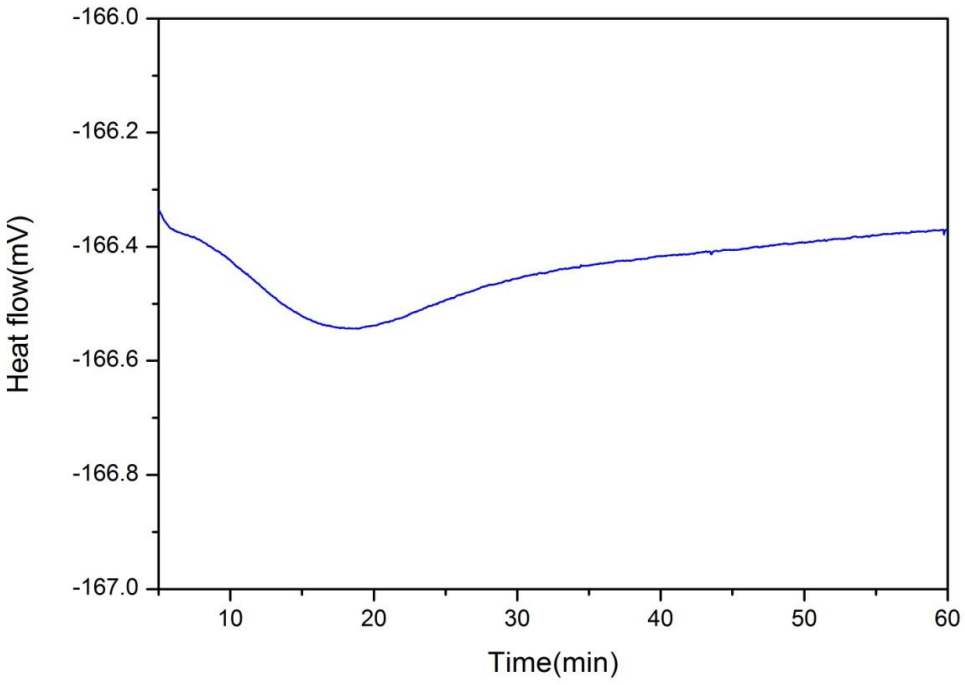

Figure 3.4.3: Simultaneous polymerisation and crystallisation of CBT at 190 ℃

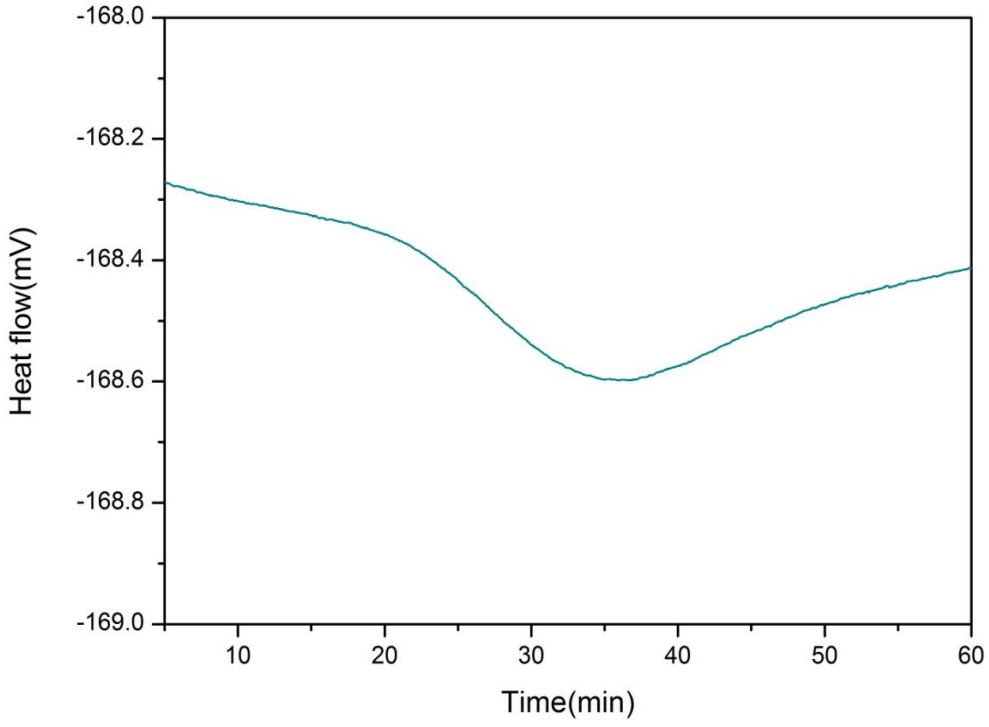

Figure 3.4.4: Simultaneous polymerisation and crystallisation of CBT at 200 ℃

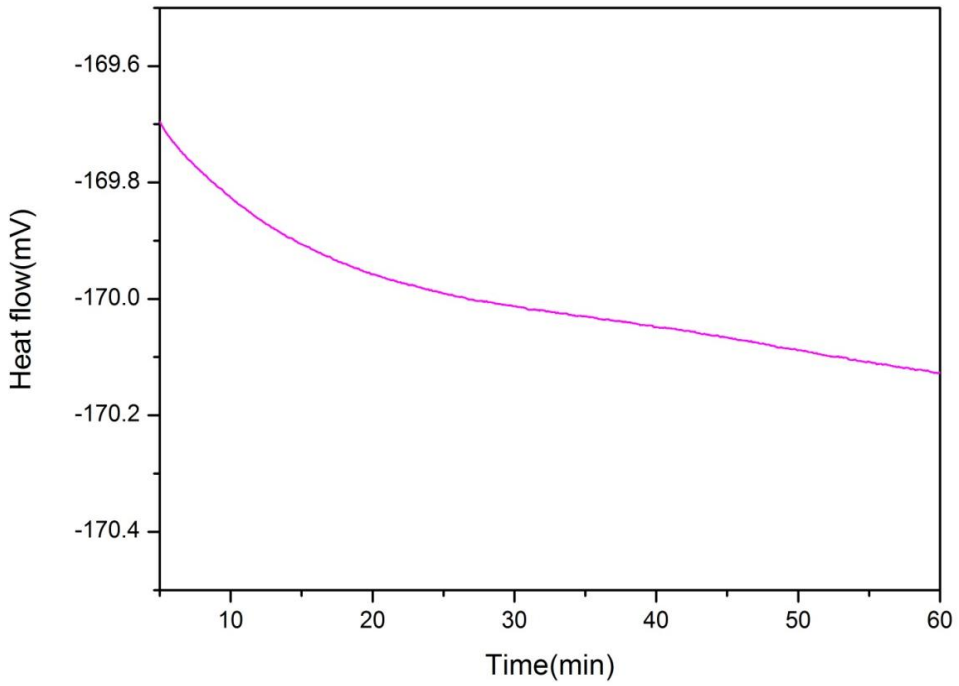

Figure 3.4.5: Simultaneous polymerisation and crystallisation of CBT at 210 ℃

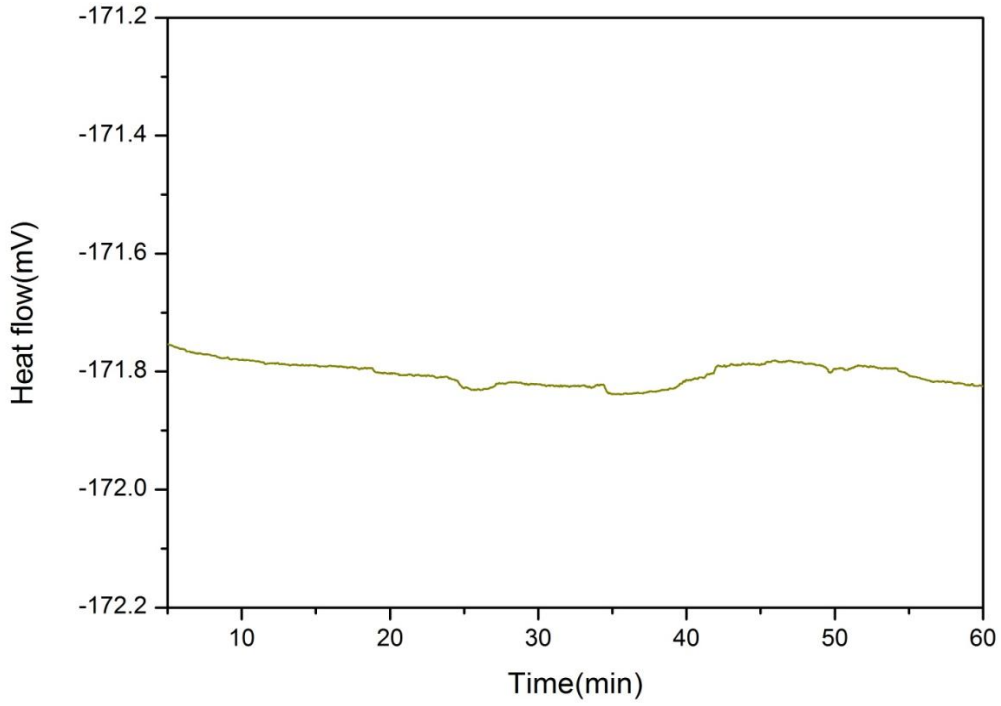

Figure 3.4.6: Simultaneous polymerisation and crystallisation of CBT at 220 ℃

It is observed that there is a dip which means a crystallisation process. From the isothermal DSC trace at 170 ℃ (Figure.3.4.1), the small dip of the crystallisation process was observed after 10 minutes. At 180 ℃ (Figure.3.4.2) the crystallite development was observed clearly after 11 minutes. The DSC trace also shows that the crystallisation process occurred after 18 minutes at 190 ℃ (Figure.3.4.3). At 200 ℃ (Figure.3.4.4), the crystallisation begin at 37min. There are no dip at 210 ℃ and 220 ℃ (Figure.3.4.5 and Figure.3.4.6). It is supposed that it takes more time for crystallisation at a higher temperature. So the faster crystallisation speed at lower temperatures is characteristic of crystalline lamellar growth during isothermal crystallisation.

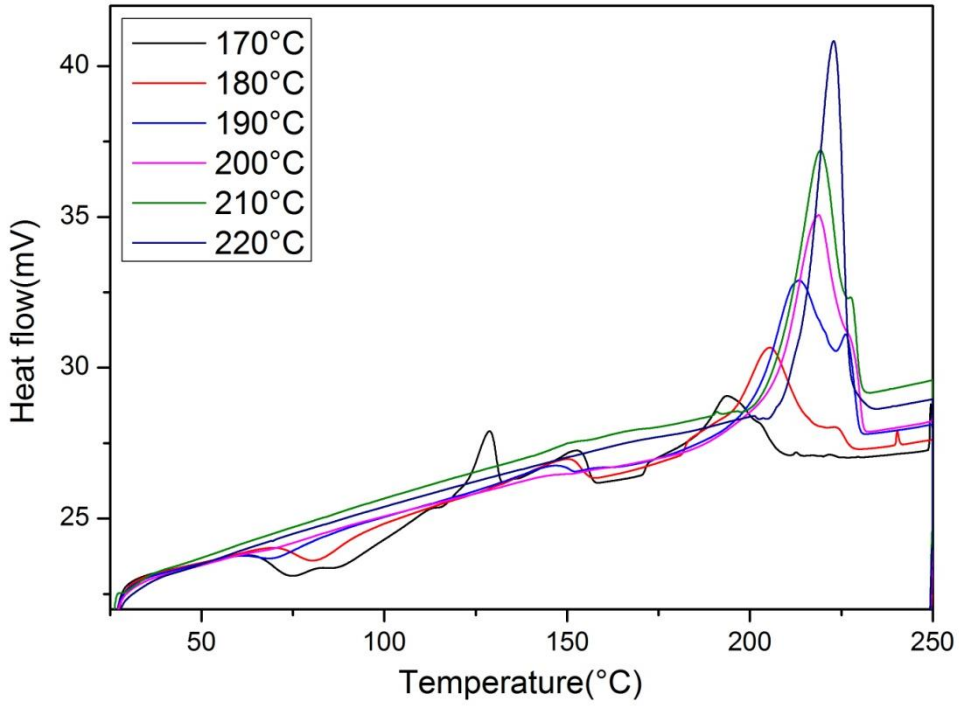

Figure 3.5: The melting point of c-PBT after simultaneous in situ polymerisation and crystallisation of CBT at various temperatures

From figure.3.5, it is obvious that there is still an oligomer melting peak from isothermal crystallisation at 170 ℃ which means polymerisation was not complete in the first run. Multiple melting peaks is usually attributed either to the presence of crystallite

populations differing in sizes or to the occurrence of a process of melting – crystallization - remelting taking place at heating [53].

Also, the T_m of polymer is affected by T_c, the higher temperature of crystallisation, the higher temperature of melting.

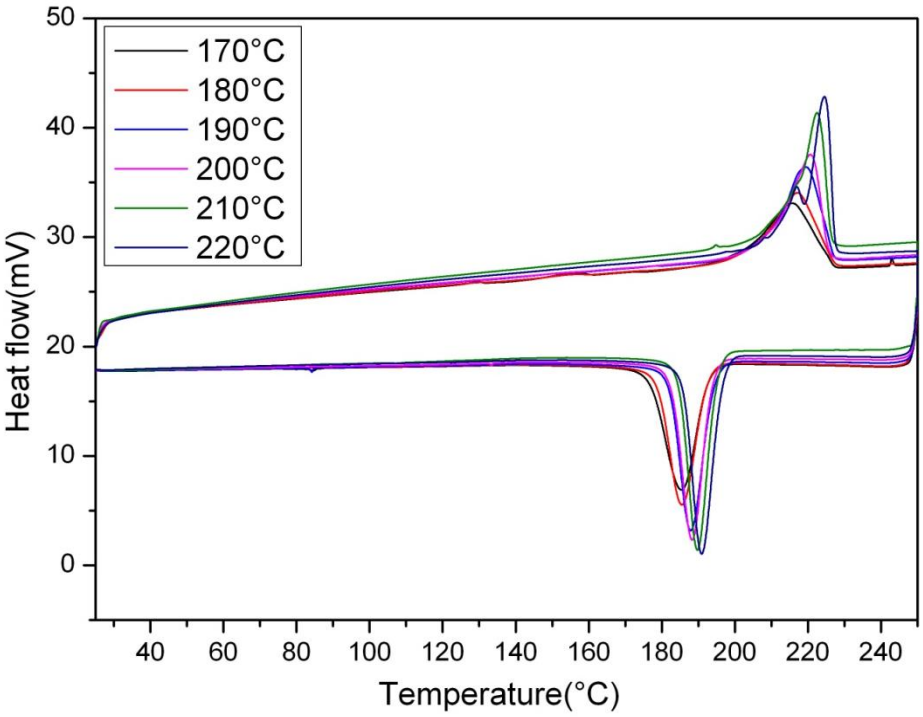

Figure 3.6: The DSC curve for third run

In the third run (Figure 3.6), no oligomer Tm is observed at170 ℃ comparing to the Figure.3.5. Moreover, double melting peak because that the crystallisation in the first isothermal step and second run was not completed. New crystallites have formed during the third step.

3.1.3 Thermal behaviour of composite

The comparison of CBT/CNTs composites is shown in Figure.3.7

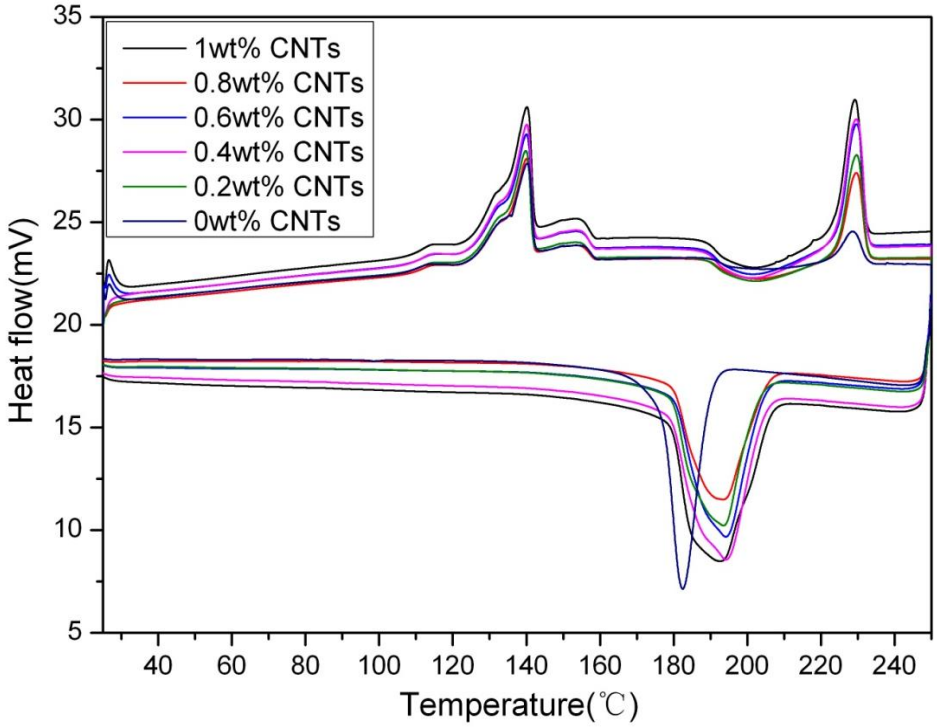

Figure 3.7: Thermal behaviour of various compositions CBT/CNTs composites

In the first run, the T_m region is clearly affected by the content of CNTs. The crystallinity increases significantly after adding the carbon nanotubes, so the presence of MWNTs appears to act as a nucleating agent.

The reheating trace of pure CBT and CBT/ carbon nanotube composites at a rate of 5 ℃ /min is shown in Figure 3.8

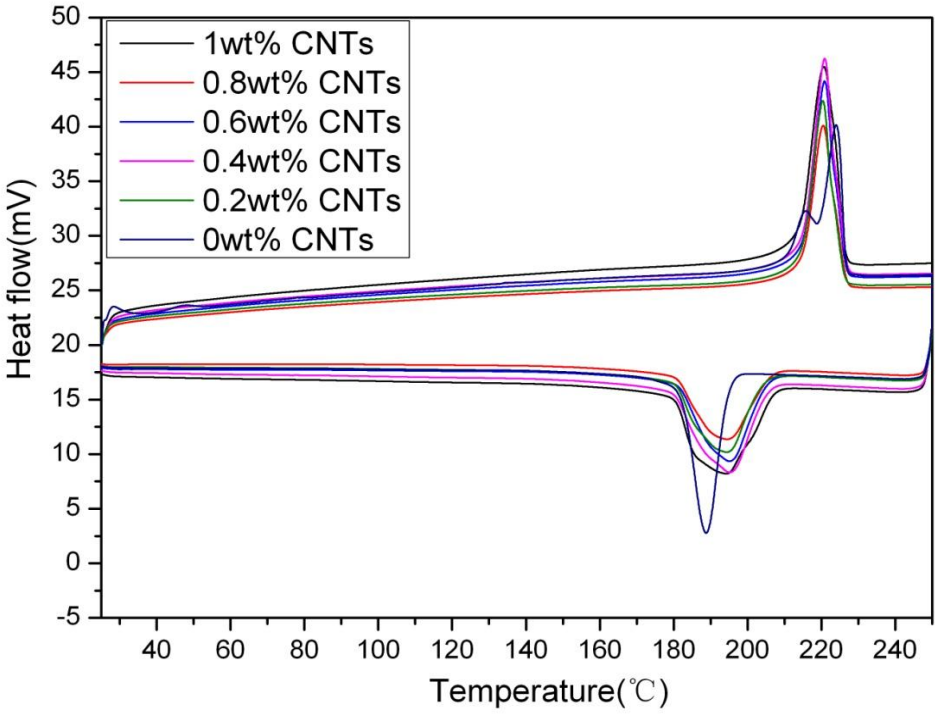

Figure 3.8: Thermal behaviour of reheating compositions CBT/CNTs composites

In the second run, the carbon nanotubes decrease the melting temperature. There is only one peak in the recrystallisation process. The recrystallisation temperature of composite is higher than that of the neat c-PBT.

The degree of crystallinity (%) of c-PBT which was formed in this study was calculated according to Equation 3.1:

$\chi_c = \Delta H / \Delta H^0 \times 100$ [54],

where ΔH is the measured (by the DSC) heat of fusion for the sample and ΔH^0 is the heat of fusion for 100% crystalline polymer. According to work published earlier [54], ΔH^0 which is used to calculate the degree of crystallinity of c-PBT as 85.75 J/g .

Table 3.1 The data of melting temperature and crystallinity

CNTs content (wt%)	Run1			Run 2		
	Melting peak(℃)	ΔH(J/g)	Crystallinity (%)	Melting peak(℃)	ΔH(J/g)	Crystallinity (%)
0	229.03	8.2	9.33	224.00	48	55.98
0.2	229.70	22.1	25.66	220.40	51.2	59.47
0.4	229.60	28.4	32.65	220.87	60.9	69.97
0.6	229.63	25.3	29.15	220.87	55.5	64.14
0.8	229.60	19.8	23.32	220.47	55.2	58.31
1	229.23	29.0	33.82	220.67	68	79.30

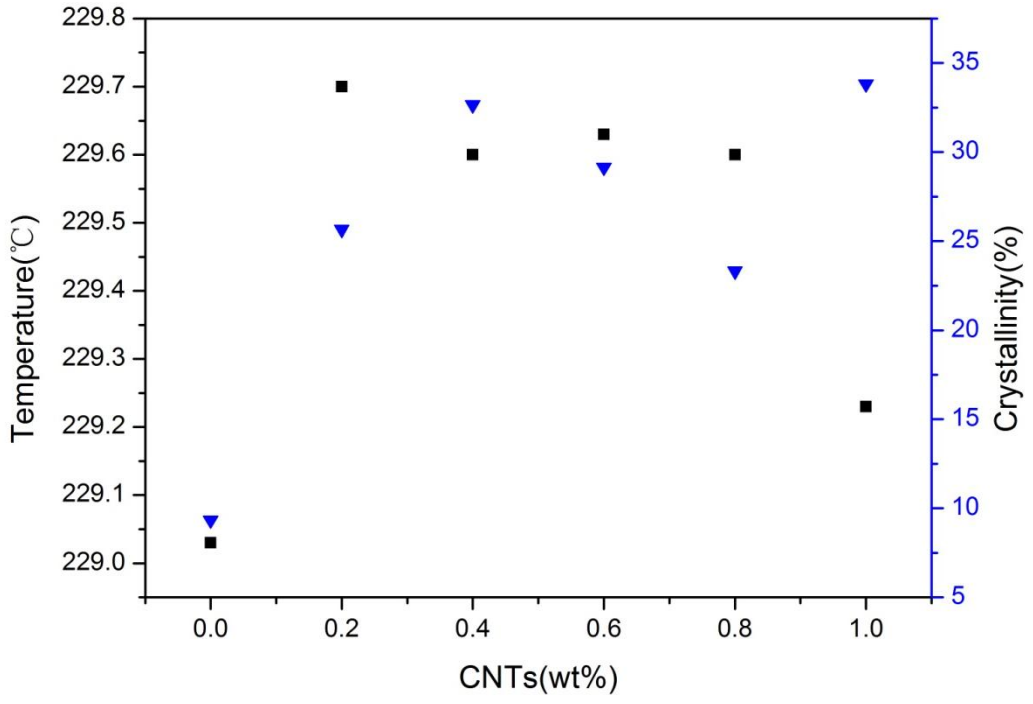

Figure 3.9: melting temperature and crystallinity of CBT/CNTs composite

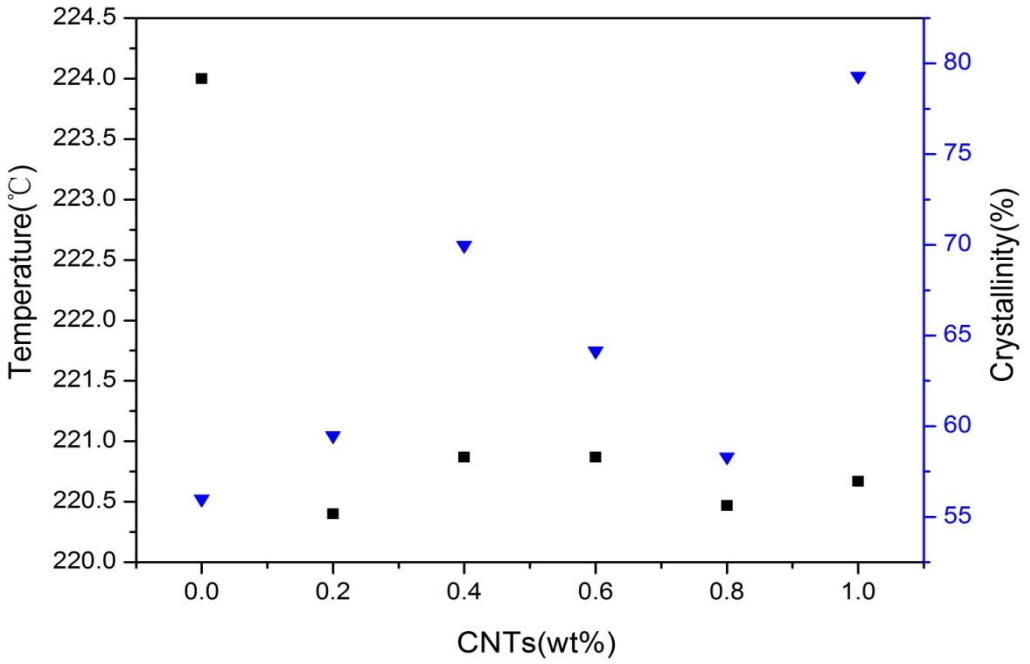

Figure 3.10: melting temperature and crystallinity of reheating CBT/CNTs composite

The exact data for peak temperature and ΔH are shown in Table 3.1. Comparing with first run and second run, the crystallinities of second run are higher than those of the first run, but the melting temperatures are 9 ℃ lower than the first run. This may because the recrystallisation and reheating process which improve the degree of crystal perfection. Furthermore, in both runs, the highest crystallinity appears at 0.4 wt% CNTs and the lowest crystallinity appears at 0.8 wt%.

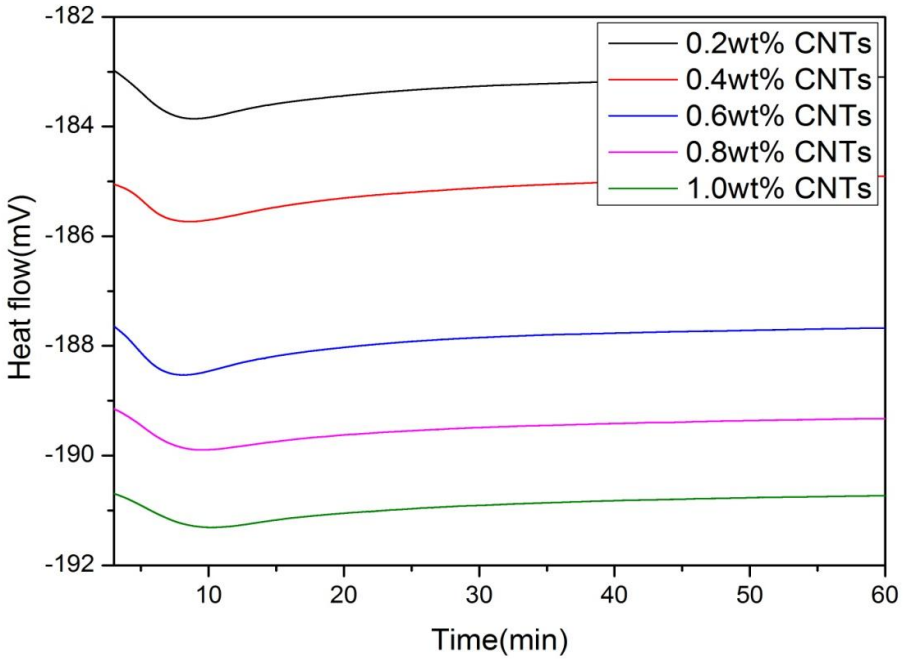

Figure 3.11: *In situ* polymerisation of CBT/CNTs composite at 190 ℃

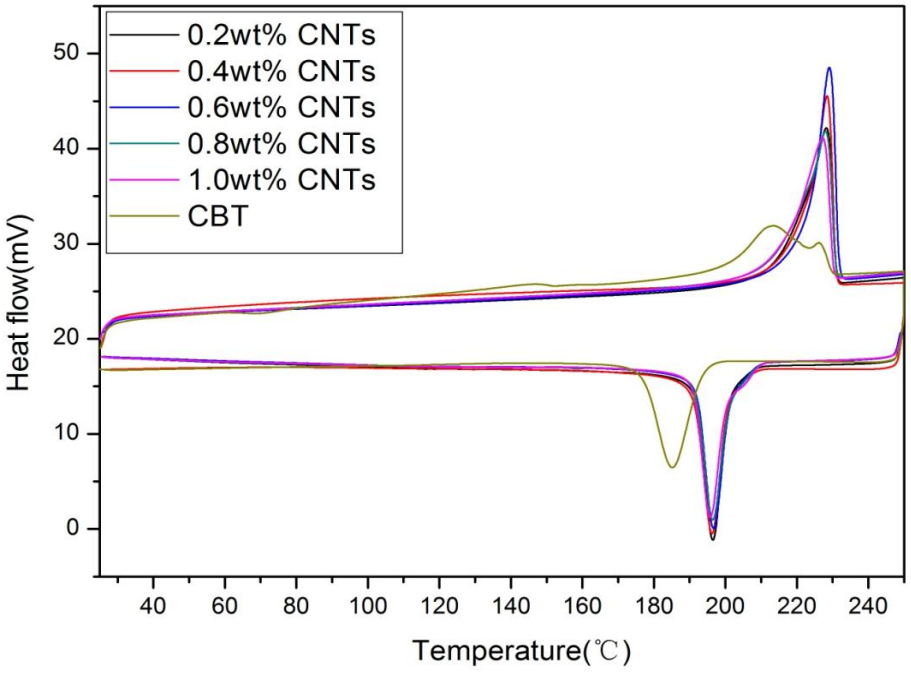

Figure 3.12: Thermal behaviour of various compositions c-PBT/CNTs composite after *in situ* polymerisation

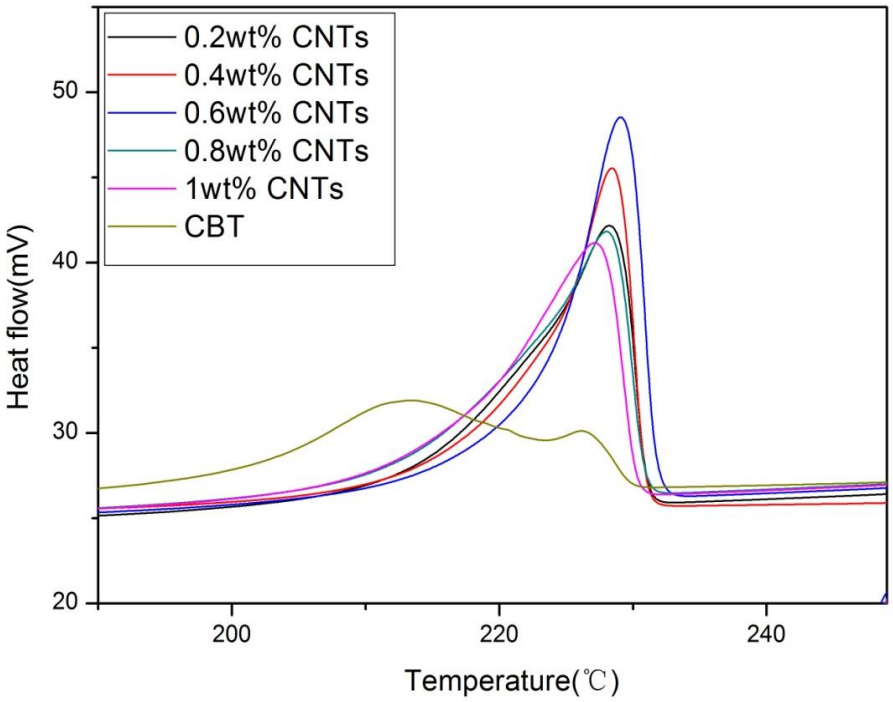

Figure 3.13: 'Close-up' of the polymer melting peak in Figure 3.11

In Figure 3.12 and 3.13, we can see that the melting peak of composites are single melting peaks but the CBT is not, so CBT could polymerise very well in the presence of CNTs in an *in situ* polymerisation process. The crystallinity increases with the content of CNTs below 0.8 wt%. This may be explained by the CNTs clumps decreasing the crystallinity.

3.2 FTIR examination

Figure 3.14 shows the whole FTIR spectra of CBT

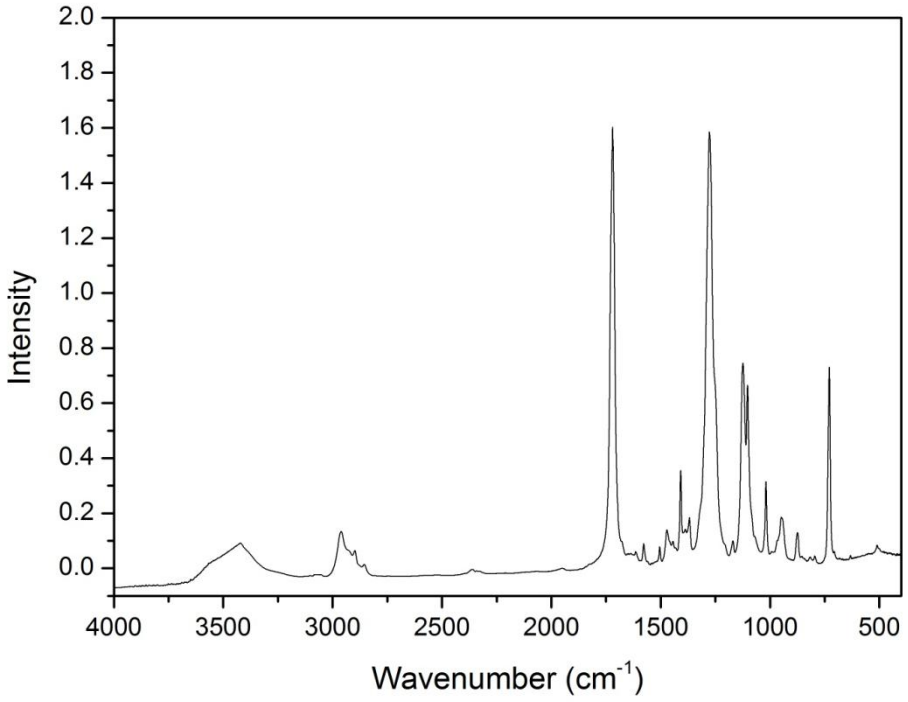

Figure 3.14: FTIR Spectra of CBT

In FTIR spectra, the following peak wavenumbers corresponding to the entire CBT structure are shown in the table below [8]:

CBT wavenumbers (cm^{-1})	Assignment
3000 to 2800	$(CH2)_4$ stretching
1750 to 1600	C=O stretching
1300 to 1100	C-O stretching
800 to 700	Benzene bending

From the FTIR spectra during the heating process, only the C-O stretching and C=O stretching band were affected, but the other peaks do not change, so the investigation focused on the ester groups which were involved in polymerisation.

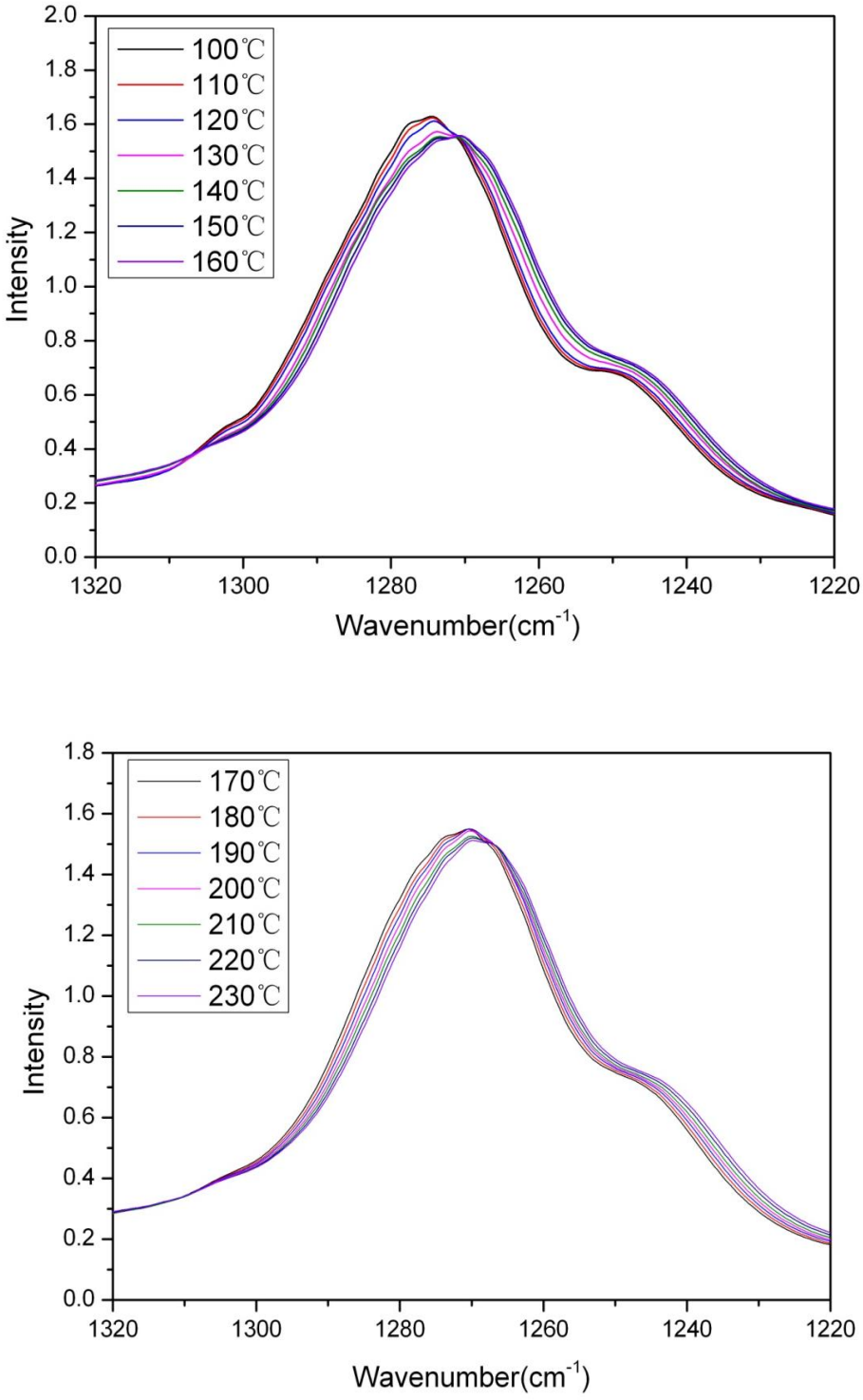

Figure 3.15: Changes in C-O *str*. band (1320 to 1220 cm^{-1}) for heating of CBT

Figure 3.15 shows the changes of C-O stretching band during polymerisation of CBT. It is observed that the peak shifts to lower wavenumber with the increase of temperature. This indicates that heating makes CBT into a more ordered structure. Increasing temperature developed crystallisation and polymerisation.

Figure 3.16 shows the changes of C=O stretching band during polymerisation of CBT. When the sample starts melting at 150 ℃, a peaks appears at 1724 cm^{-1}. At start, the peak around 1724 cm^{-1} is smaller than that around 1720 cm^{-1}. As temperature increases, the peak around 1724 cm^{-1} wavenumber becomes bigger than that 1720 cm^{-1}. In the region of CBT melting (150 ℃-170 ℃), the appearance of a peak around 1724 cm^{-1} wavenumber suggests that the chemical structure of C=O stretching band changed during the polymerisation. These changes suggest that CBT ring expansion polymerisation occurs at this region. When the temperature above 180 ℃, the intensity around 1724 cm^{-1} wavenumber becomes larger than1720 cm^{-1}. It was expected crystal forms in this region. So before CBT melting, the polymer is amorphous. After heating, crystallisation and polymerisation occur and finally the material forms the semi-crystalline polymer.

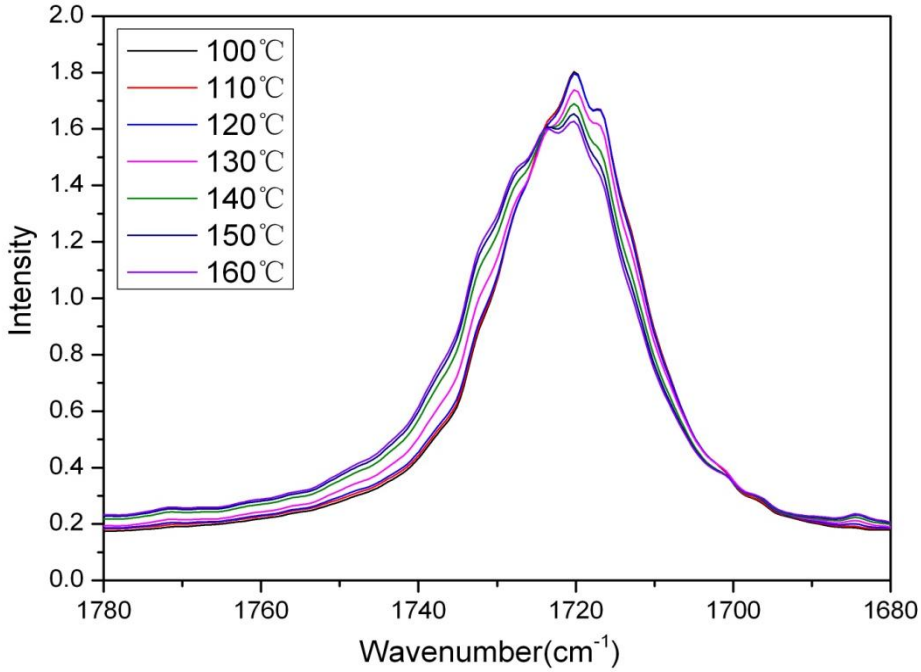

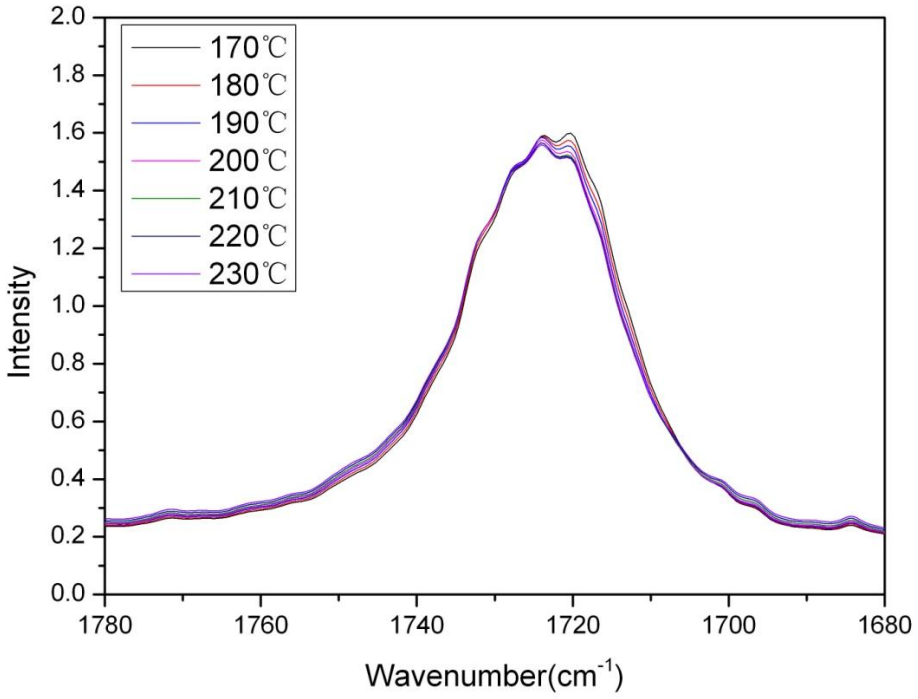

Figure 3.16: Changes in C=O *str.* band (1780 to 1680 cm^{-1}) for heating of CBT

3.3 Raman spectroscopy

Fig 3.17 illustrates the Raman spectra of CBT, CNTs and composites. It is clear that there are two peaks at ~1320 cm^{-1} (D band) and ~1580 cm^{-1} (G band). G band is related to the defects or disordered structure in tubes. It can be seen that two small peaks at 1320 cm^{-1} and 1580 cm^{-1}, so it probable that there are carbon nanotubes in the composites.

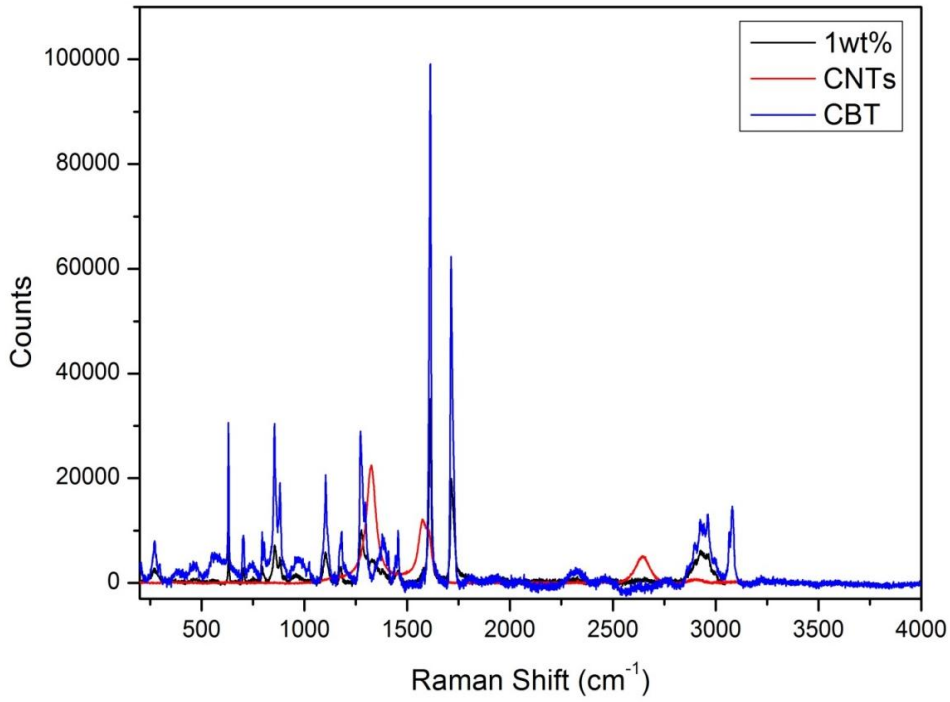

Figure 3.17: Raman spectra of CBT, CNTs and CBT/CNTs composites

3.4 Mechanical properties

In table 3.2, SD stands for standard deviation, E stands for Young's modulus, and H stands for hardness, but polymers are viscoelastic, so the 'hardness' does not like the hardness in metal.

Table 3.2 Data for Young's module and 'hardness'

Sample	E(GPa)	SD(E)	H(GPa)	SD(H)
CBT	2.90	0.124	0.17	0.010
0.2wt% CNTs	2.32	0.122	0.22	0.030
0.4wt% CNTs	2.20	0.074	0.20	0.010
0.6wt% CNTs	1.16	0.005	0.14	0.007
0.8wt% CNTs	2.55	0.151	0.21	0.013
1.0wt% CNTs	1.02	0.123	0.13	0.011

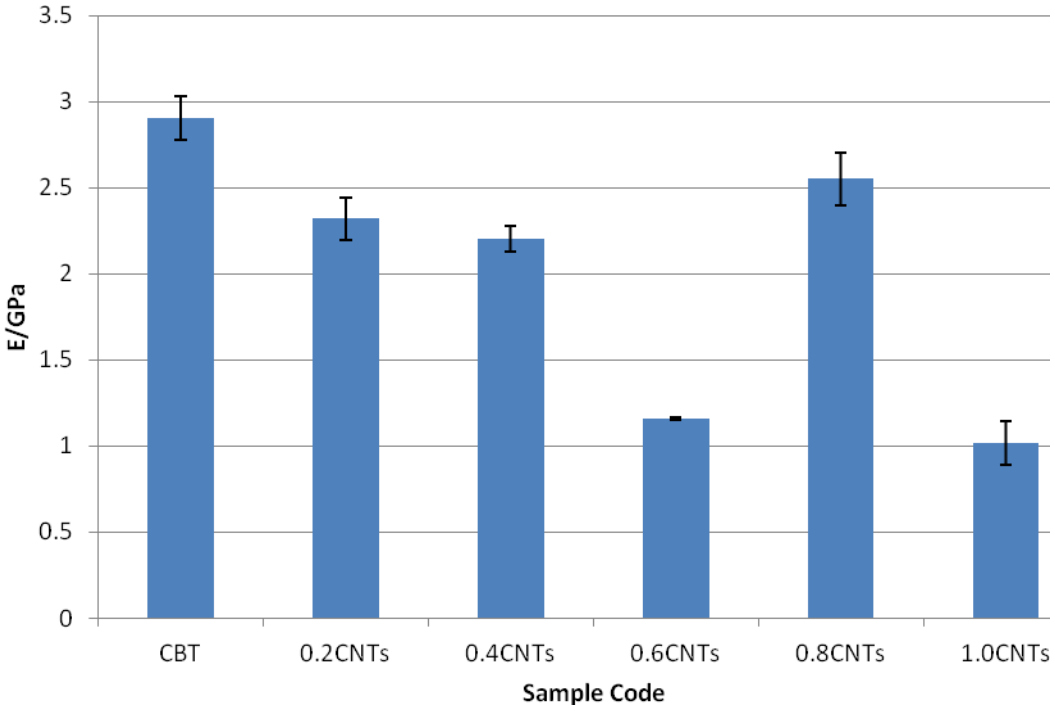

Figure 3.18 Young's module of CBT and CBT/CNTscomposites

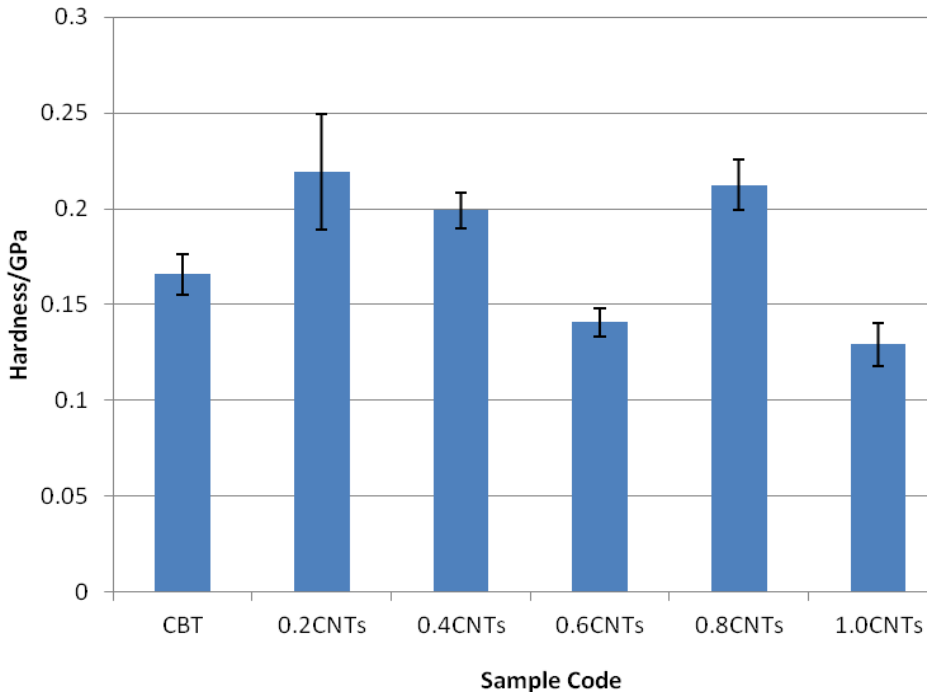

Figure 3.19 'Hardness' of CBT and CBT/CNTs composites

The results show that all the samples are very weak. The composites are less stiff than unfilled CBT. This may because that the crystal decreases the Young's modulus. Also the 0.8 wt% CNTs composite has the highest Young's modulus of the composites.

3.5 Dispersion of the MWNTs in the nanocomposites

SEM was carried out to observe the dispersion of the MWNTs in the obtained nanocomposites. Figure 3.20-3.25 show the SEM images of fractured surfaces in liquid nitrogen for the PBT/MWNT nanocomposites.

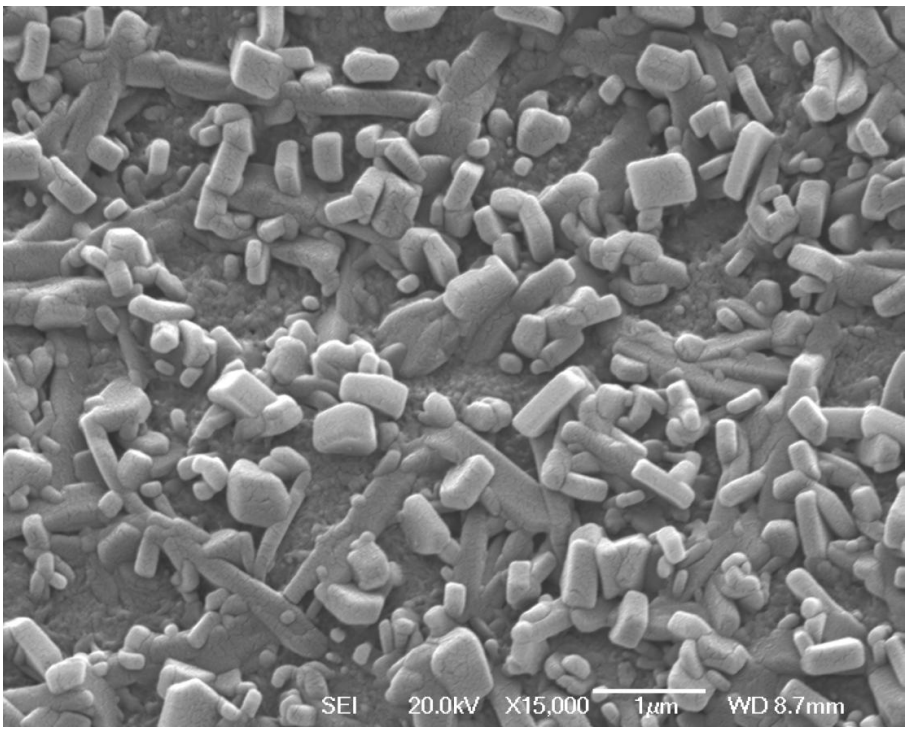

Figure 3.20: Fractured surfaces of CBT without carbon nanotubes

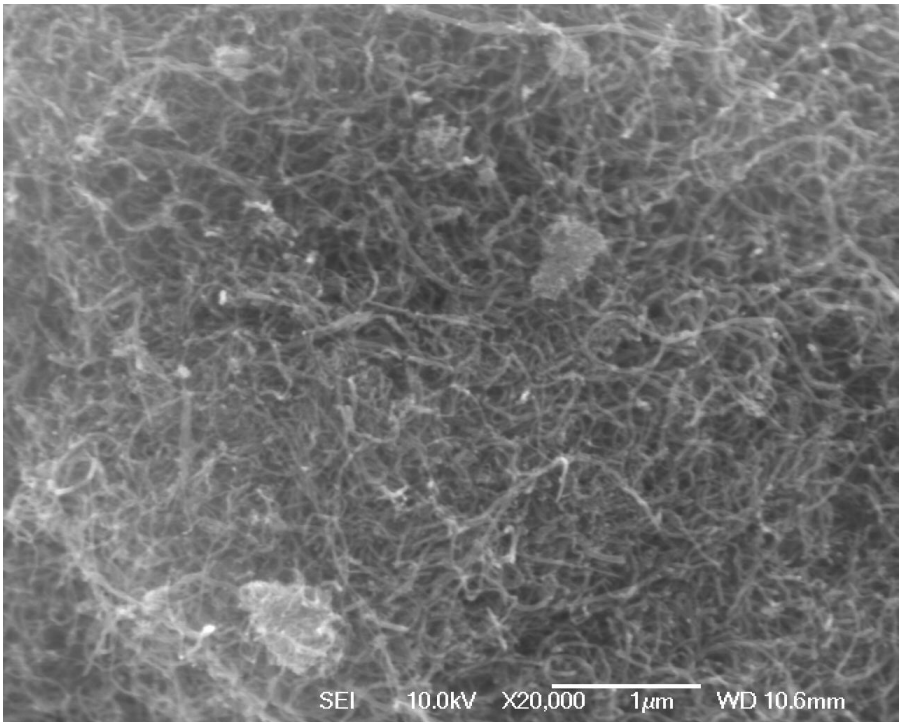

Figure 3.21: SEM image of pure carbon nanotubes

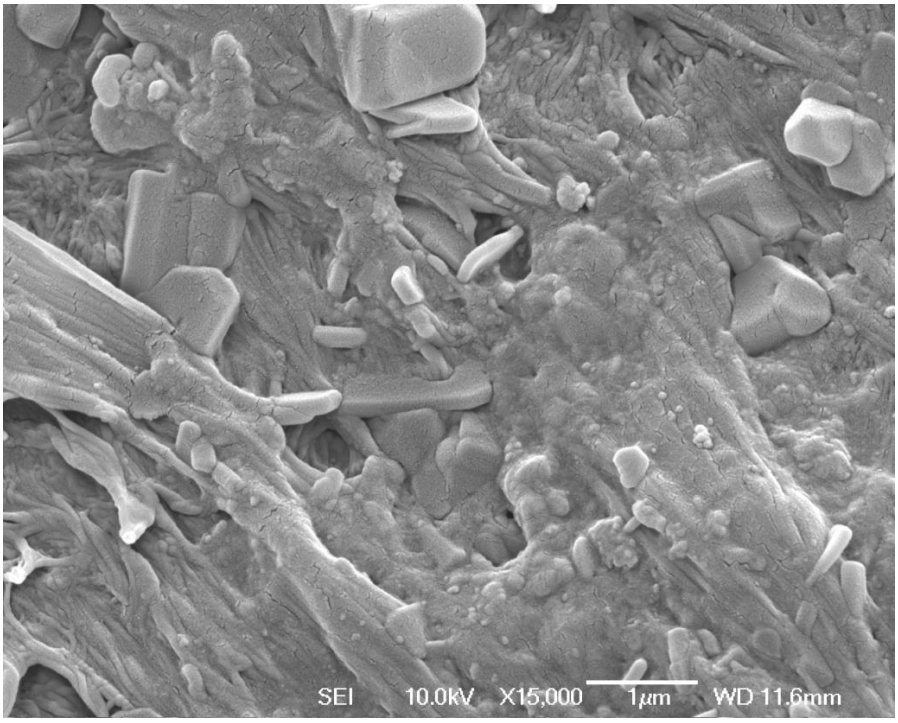

Figure 3.22: Fractured surfaces of CBT/ 0.2 wt% CNTs composite

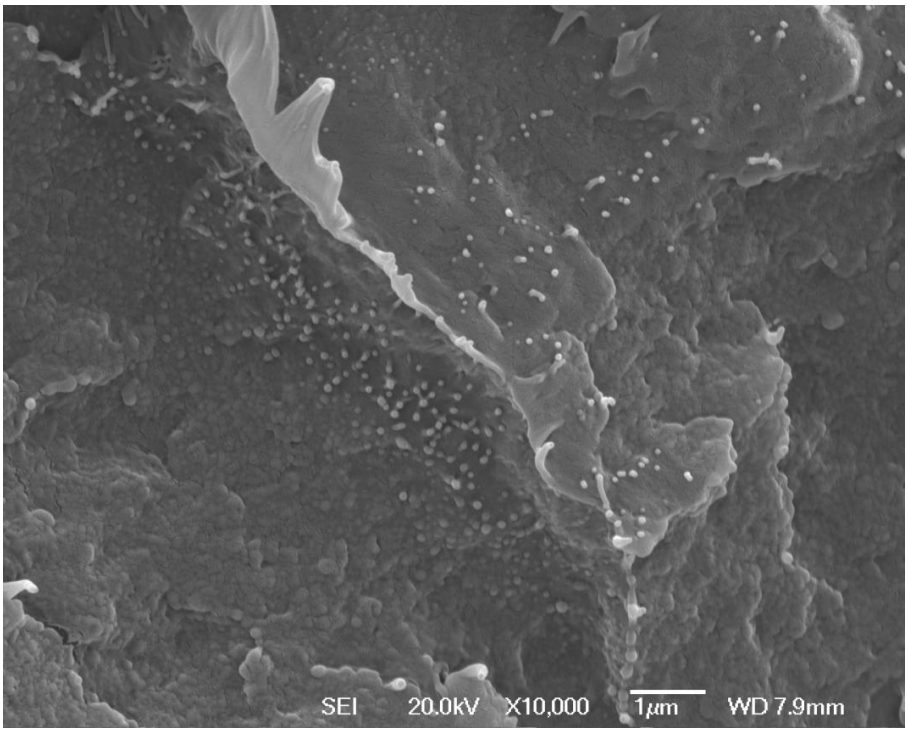

Figure 3.23: Fractured surfaces of CBT/ 0.4 wt% CNTs composite

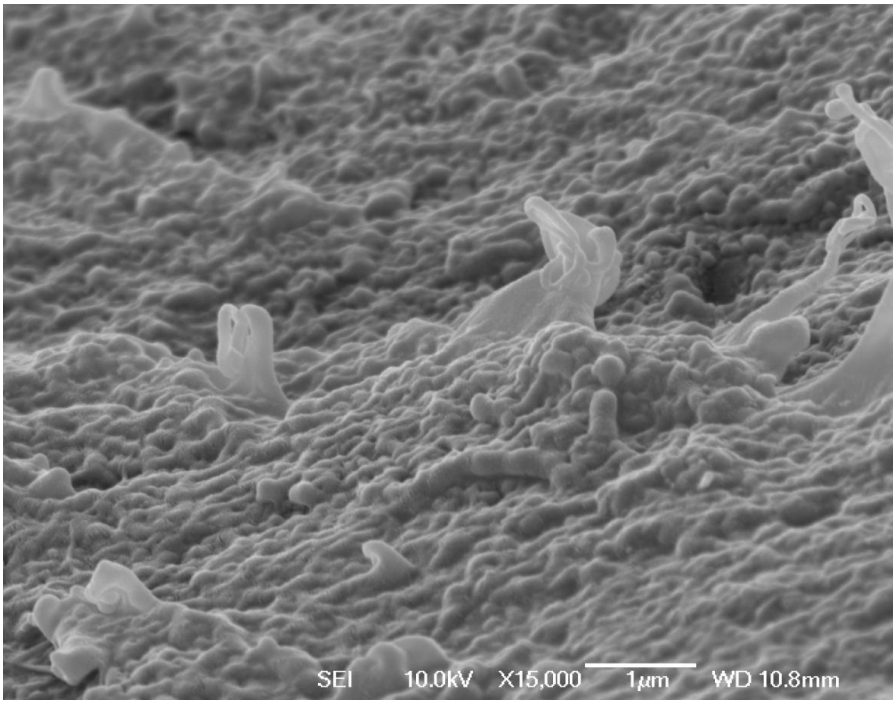

Figure 3.24: Fractured surfaces of CBT/ 0.6 wt% CNTs composite

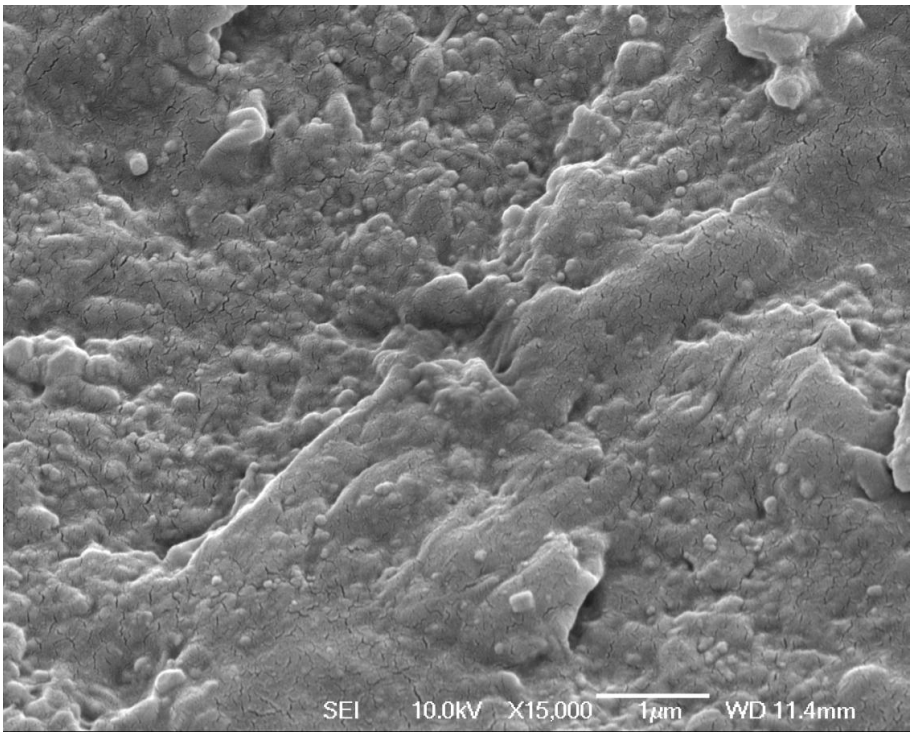

Figure 3.25: Fractured surfaces of CBT/ 0.8 wt% CNTs composite

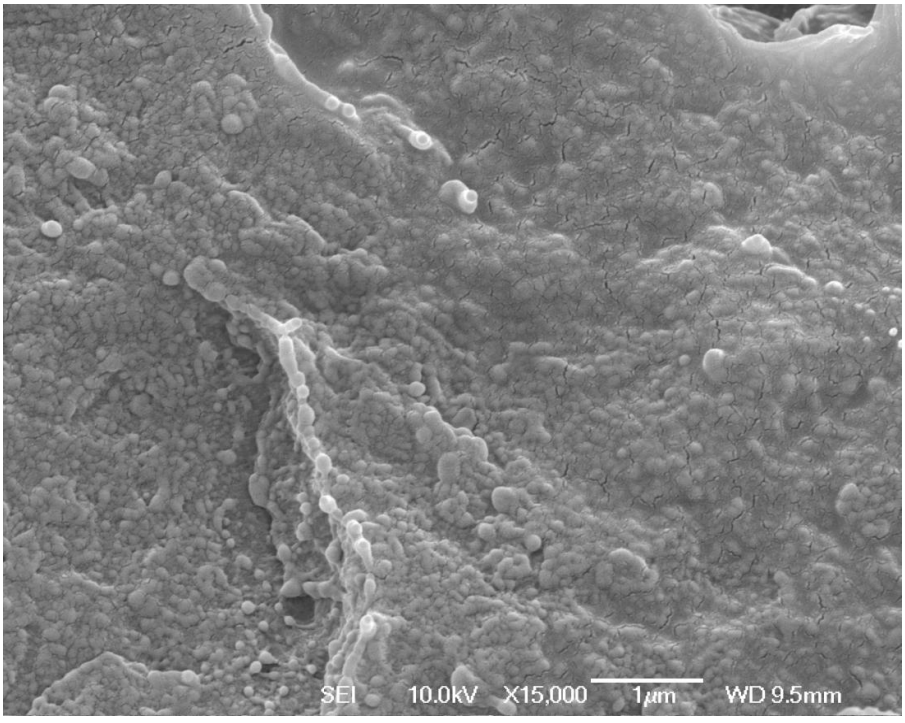

Figure 3.26: Fractured surfaces of CBT/ 1.0 wt% CNTs composite

Big aggregation or entanglement was not observed in pictures above. Generally most of the MWNTs were homogeneously dispersed in the polymer matrix. It is assumed some small entanglement when the carbon nanotube proportion over 0.8 wt% according to thermal analysis.

CHAPTER FOUR

CONCLUSION AND FURTHER WORK

4.1 Conclusion

The properties of Cyclic Poly(butylene terephthalate)/ Multiwalled Carbon Nanotube Nanocomposites have been carried out by DSC, FTIR, Raman spectroscopy, Nanoindentation and SEM.

(1) It is believed that the polymerisation of CBT is an almost thermo-neutral reaction. The polymerisation and crystallisation of c-PBT occurs simultaneously and rapidly in a short time.

(2) The faster crystallisation speed at lower temperatures. Multiple melting peaks when the polymerisation of CBT is not complete is believed to be due to the existence of mixed spherulites as a consequence of mixed cyclic and linear structures.

(3) The crystallinity increases significantly after adding the carbon nanotubes, so the presence of MWNTs acts as a nuclear agent.

(4) The highest crystallinity appears at 0.4 wt% CNTs and the lowest crystllinity appears at 0.8wt%. This may be that too much CNTs clumps decreasing the crystallinity.

(5) The Young modulus of CBT is very low compared with metal, but the addition of carbon nanotubes makes the Young modulus of the composite even smaller than pure CBT.

4.2 Further work

Since the low melting viscosity gave CBT a promising future, there is still a great deal of structure-property that needs to be understood in the applications of the material. To fully advance scientific understanding, some future work is suggested and outlined below.

(1) Due to the size of carbon nanotubes CBT and the resolution of SEM in this project, it is suggested to use TEM so the despersion of nanotubes may be observed more clearly.

(2) Only CBT/ MWNTs composites were focused on in this study. It would be interesting that nano-composites blend with other filler, such as fiber or graphite.

(3) To investigate different approaches mixing the composite, this project uses solid phase dispersion. It may be possible to blend CBT by liquid-liquid phase separation of *in situ* polymerising.

REFERENCE

[1] Pounder, Ryan J., and Andrew P. Dove. "Towards poly (ester) nanoparticles: recent advances in the synthesis of functional poly (ester) s by ring-opening polymerization." *Polymer Chemistry* 1.3 (2010): 260-271.

[2] Silvers, Angela L., Chia‐Chih Chang, and Todd Emrick. "Functional aliphatic polyesters and nanoparticles prepared by organocatalysis and orthogonal grafting chemistry." *Journal of Polymer Science Part A: Polymer Chemistry* 50.17 (2012): 3517-3529.

[3] Fox, Megan E., Francis C. Szoka, and Jean MJ Fréchet. "Soluble polymer carriers for the treatment of cancer: the importance of molecular architecture."*Accounts of chemical research* 42.8 (2009): 1141-1151.

[4] Bielawski, Christopher W., Diego Benitez, and Robert H. Grubbs. "Synthesis of cyclic polybutadiene via ring-opening metathesis polymerization: the importance of removing trace linear contaminants." *Journal of the American Chemical Society* 125.28 (2003): 8424-8425.

[5] Baets, Joris, et al. "Toughening of isothermally polymerized cyclic butylene terephthalate for use in composites." *Polymer Degradation and Stability* 95.3 (2010): 346-352.

[6] Mäder, Edith, et al. "Investigation on adhesion, interphases, and failure behaviour of cyclic butylene terephthalate (CBT®)/glass fiber composites." *Composites Science and Technology* 67.15 (2007): 3140-3150.

[7] Ishak, Z. A., K. G. Gatos, and J. Karger‐Kocsis. "On the in‐situ polymerization of cyclic butylene terephthalate oligomers: DSC and rheological studies." *Polymer Engineering & Science* 46.6 (2006): 743-750.

[8] Samsudin, Sani Amril. *The thermal behaviour and isothermal crystallisation of cyclic poly (butylene terephthalate) and its blends*. Diss. University of Birmingham, 2010.

[9] Gallucci, R. R., and B. R. Patel. "Poly (butylene terephthalate)." *Modern Polyesters: Chemistry and Technology of Polyesters and Copolyesters* (2004): 293-321.

[10] Baets, Joris, et al. "Toughening of polymerized cyclic butylene terephthalate with carbon nanotubes for use in composites." *Composites Part A: Applied Science and Manufacturing* 39.11 (2008): 1756-1761.

[11] Romhány, Gábor, et al. "pCBT/MWCNT Nanocomposites Prepared by In situ Polymerization of CBT after Solid‐Phase High‐Energy Ball Milling of CBT with MWCNT." *Macromolecular Materials and Engineering* 296.6 (2011): 544-550.

[12] Balogh, Gábor, et al. "Preparation and characterization of in situ polymerized cyclic butylene terephthalate/graphene nanocomposites." *Journal of Materials Science* 48.6 (2013): 2530-2535.

[13] Fabbri, Paola, et al. "Preparation and characterization of poly (butylene terephthalate)/ graphene composites by in-situ polymerization of cyclic butylene terephthalate." *Polymer* 53.4 (2012): 897-902.

[14] Matthews, Alice. *Thermal characterisation of XB2-CA4: cyclic poly (butylene terephthalate) with stannoxane catalyst*. Diss. University of Birmingham, 2010.

[15] Espinoza-Martínez, Adriana, et al. "Nucleation mechanisms of aromatic polyesters, PET, PBT, and PEN, on single-wall carbon nanotubes: early nucleation stages." *Journal of Nanomaterials* 2012 (2012): 98.

[16] Kasaliwal, Gaurav R., et al. "Analysis of agglomerate dispersion mechanisms of multiwalled carbon nanotubes during melt mixing in polycarbonate." *Polymer* 51.12 (2010): 2708-2720.

[17] De Volder, Michael FL, et al. "Carbon nanotubes: present and future commercial applications." *Science* 339.6119 (2013): 535-539.

[18] Vairavapandian, Deepa, Pornnipa Vichchulada, and Marcus D. Lay. "Preparation and modification of carbon nanotubes: review of recent advances and applications in catalysis and sensing." *Analytica chimica acta* 626.2 (2008): 119-129.

[19] Thostenson, Erik T., Zhifeng Ren, and Tsu-Wei Chou. "Advances in the science and technology of carbon nanotubes and their composites: a review." *Composites science and technology* 61.13 (2001): 1899-1912.

[20] Harris, Peter JF, and Peter John Frederich Harris. *Carbon nanotube science: synthesis, properties and applications*. Cambridge University Press, 2009.

[21] http://spectrum.ieee.org/nanoclast/semiconductors/nanotechnology/carbon-nanotube-supply-glut-claims-its-first-victim

[22] Mandal, Amit, and Arun K. Nandi. "Noncovalent functionalization of multiwalled carbon nanotube by a polythiophene-based compatibilizer: reinforcement and conductivity improvement in poly (vinylidene fluoride) films." *The Journal of Physical Chemistry C* 116.16 (2012): 9360-9371.

[23] Huang, Xingyi, et al. "Influence of aspect ratio of carbon nanotubes on crystalline phases and dielectric properties of poly (vinylidene fluoride)."*European Polymer Journal* 45.2 (2009): 377-386.

[24] Özdilek, Ceren, et al. "Thermally induced phase separation in PαMSAN/PMMA blends in presence of functionalized multiwall carbon nanotubes: Rheology, morphology and electrical conductivity." *Polymer* 52.20 (2011): 4480-4489.

[25] Wu, Defeng, et al. "Crystallization and thermal behavior of multiwalled carbon nanotube/poly (butylenes terephthalate) composites." *Polymer Engineering & Science* 48.6 (2008): 1057-1067.

[26] Wu, Fangjuan, and Guisheng Yang. "Synthesis and properties of poly (butylene terephthalate)/multiwalled carbon nanotube nanocomposites prepared by in situ polymerization and in situ compatibilization." *Journal of applied polymer science*118.5 (2010): 2929-2938.

[27] Sperling, Leslie Howard. *Introduction to physical polymer science*. John Wiley & Sons, 2005.

[28] Bal, Smrutisikha. "Dispersion and reinforcing mechanism of carbon nanotubes in epoxy nanocomposites." *Bulletin of Materials Science* 33.1 (2010): 27-31.

[29] Garg, Paritosh, et al. "An experimental study on the effect of ultrasonication on viscosity and heat transfer performance of multi-wall carbon nanotube-based aqueous nanofluids." *International Journal of Heat and Mass Transfer* 52.21 (2009): 5090-5101.

[30] Ma, Peng-Cheng, et al. "Dispersion and functionalization of carbon nanotubes for polymer-based nanocomposites: a review." *Composites Part A: Applied Science and Manufacturing* 41.10 (2010): 1345-1367.

[31] Kim, Y. A., et al. "Effect of ball milling on morphology of cup-stacked carbon nanotubes." *Chemical physics letters* 355.3 (2002): 279-284.

[32] Wang, Hailian, and Ru Xiao. "Preparation and characterization of CNTs/PE micro‐nanofibers." *Polymers for Advanced Technologies* 23.3 (2012): 508-515.

[33] Spitalsky, Zdenko, et al. "Carbon nanotube–polymer composites: chemistry, processing, mechanical and electrical properties." *Progress in Polymer Science*35.3 (2010): 357-401.

[34] Chang, Chih-Wei, et al. "Thermal decomposition of carbon nanotube/Al_2O_3 powders by DSC testing." *Composites Science and Technology* 68.14 (2008): 2954-2959.

[35] Sobolkina, Anastasia, et al. "Dispersion of carbon nanotubes and its influence on the mechanical properties of the cement matrix." *Cement and Concrete Composites* 34.10 (2012): 1104-1113.

[36] Xie, Xiao-Lin, Yiu-Wing Mai, and Xing-Ping Zhou. "Dispersion and alignment of carbon nanotubes in polymer matrix: a review." *Materials Science and Engineering: R: Reports* 49.4 (2005): 89-112.

[37] Vasconcelos, Teofilo, Bruno Sarmento, and Paulo Costa. "Solid dispersions as strategy to improve oral bioavailability of poor water soluble drugs." *Drug discovery today* 12.23 (2007): 1068-1075.

[38] http://www.cyclics.com/composites

[39] http://www.cheaptubes.com/

[40] Lehmann, B., and J. Karger-Kocsis. "Isothermal and non-isothermal crystallisation kinetics of pCBT and PBT." *Journal of Thermal Analysis and Calorimetry* 95.1 (2009): 221-227.

[41] Bruylants, Gilles, Johan Wouters, and Catherine Michaux. "Differential scanning calorimetry in life science: thermodynamics, stability, molecular recognition and application in drug design." *Current medicinal chemistry* 12.17 (2005): 2011-2020.

[42] Hatakeyama, T., and F. X. Quinn. "Fundamentals and applications to polymer science." *Thermal Analysis* (1994).

[43] Bell, Robert. *Introductory Fourier transform spectroscopy*. Elsevier, 2012.

[44] Lerma-García, M. J., et al. "Authentication of extra virgin olive oils by Fourier-transform infrared spectroscopy." *Food Chemistry* 118.1 (2010): 78-83.

[45] Griffiths, Peter R., and James A. De Haseth. *Fourier transform infrared spectrometry*. Vol. 171. John Wiley & Sons, 2007.

[46] Ferrari, A. C., and J. Robertson. "Interpretation of Raman spectra of disordered and amorphous carbon." *Physical review B* 61.20 (2000): 14095.

[47] Wikipedia

[48] Dresselhaus, Mildred S., et al. "Raman spectroscopy of carbon nanotubes."*Physics Reports* 409.2 (2005): 47-99.

[49] Ferrari, A. C., and J. Robertson. "Interpretation of Raman spectra of disordered and amorphous carbon." *Physical review B* 61.20 (2000): 14095.

[50] Calleja, FJ Baltá, and Stoyko Fakirov. *Microhardness of polymers*. Cambridge University Press, 2007.

[51] Oyen, Michelle L., and Robert F. Cook. "A practical guide for analysis of nanoindentation data." *Journal of the mechanical behavior of biomedical materials* 2.4 (2009): 396-407.

[52] Reimer, Ludwig. *Scanning electron microscopy: physics of image formation a. microanalysis*. Berlin etc: Springer, 1998.

[53] González-Vidal, Nathalie, et al. "Synthesis and properties of poly (hexamethylene terephthalate)/multiwall carbon nanotubes nanocomposites." *Composites Science and Technology* 70.5 (2010): 789-796.

[54] Parton, Hilde, et al. "Properties of poly (butylene terephthatlate) polymerized from cyclic oligomers and its composites." *Polymer* 46.23 (2005): 9871-9880.